DESIGN AND SYNTHESIS OF MODIFIED CHITOSAN/COLLAGEN COATED-GOLD

NANOPARTICLES AS A CARRIER FOR ANTICANCER AND ANTIINFLAMMATORY AGENTS

Miss Naruthai Hongsa

จุฬาลงกรณ์มหาวิทยาลัย
CHULALONGKORN UNIVERSITY

A Thesis Submitted in Partial Fulfillment of the Requirements

for the Degree of Master of Science in Chemistry

Department of Chemistry

FACULTY OF SCIENCE

Chulalongkorn University

Academic Year 2020

การออกแบบและสังเคราะห์อนุภาคทองคำระดับนาโนเมตรที่เคลือบด้วยไคโตซานดัดแปร/คอลลาเจน
เพื่อเป็นตัวนำส่งสำหรับสารยับยั้งมะเร็งและสารต้านการอักเสบ

น.ส.นฤทัย หงษ์สา

Thesis Title	DESIGN AND SYNTHESIS OF MODIFIED CHITOSAN/COLLAGEN COATED-GOLD NANOPARTICLES AS A CARRIER FOR ANTICANCER AND ANTIINFLAMMATORY AGENTS
By	Miss Naruthai Hongsa
Field of Study	Chemistry
Thesis Advisor	Professor NONGNUJ MUANGSIN, Ph.D.
Thesis Co Advisor	Kanokwan Sansanaphongpricha, Ph.D.

Accepted by the FACULTY OF SCIENCE, Chulalongkorn University in Partial Fulfillment of the Requirement for the Master of Science

-- Dean of the FACULTY OF SCIENCE

(Professor POLKIT SANGVANICH, Ph.D.)

THESIS COMMITTEE

-- Chairman

(Professor VUDHICHAI PARASUK, Ph.D.)

-- Thesis Advisor

(Professor NONGNUJ MUANGSIN, Ph.D.)

-- Thesis Co-Advisor

(Kanokwan Sansanaphongpricha, Ph.D.)

-- Examiner

(Professor THAWATCHAI TUNTULANI, Ph.D.)

-- External Examiner

(Assistant Professor Kittipong Chainok, Ph.D.)

นฤทัย หงษ์สา : การออกแบบและสังเคราะห์อนุภาคทองคำระดับนาโนเมตรที่เคลือบด้วยไคโต
ซานดัดแปร/คอลลาเจนเพื่อเป็นตัวนำส่งสำหรับสารยับยั้งมะเร็งและสารต้านการอักเสบ. (
DESIGN AND SYNTHESIS OF MODIFIED CHITOSAN/COLLAGEN COATED-GOLD
NANOPARTICLES AS A CARRIER FOR ANTICANCER AND ANTIINFLAMMATORY
AGENTS) อ.ที่ปรึกษาหลัก : ศ. ดร.นงนุช เหมืองสิน, อ.ที่ปรึกษาร่วม : ดร.กนกวรรณ ศันสนะ
พงษ์ปรีชา

ในงานวิจัยนี้มีจุดประสงค์เพื่อพัฒนาประสิทธิภาพในการนำส่งของ AuNPs ซึ่งหนึ่งในปัญหา
ของการบรรจุยาและการสลายตัวของยาคือ ยาถูกบรรจุลงในบนพื้นผิวของอนุภาคทองคำจะมีการเกาะ
บริเวณรอบนอกของพื้นผิวซึ่งง่ายต่อการสลายตัวเมื่ออยู่ในสภาวะภายในของร่างกาย ดังนั้นเราจึงพัฒนา
AuNPs ด้วยการเคลือบพื้นผิวของอนุภาคทองคำด้วยด้วยไคโตซานดัดแปร (Bi-QCS) ซึ่งอนุภาคทองคำดัด
แปรไคโตซาน/คอลลาเจน (Bi-QCS-AuNPS@collagen) ได้รับการออกแบบดังนี้: (i) คอลลาเจนถูกใช้เป็น
ตัวรีดิวซ์และเป็นสารสร้างความเสถียรเบื้องต้นให้กับอนุภาคทองคำ(AuNPs@collagen) ในขณะที่ (ii)
พอลิเมอร์ที่มีประจุบวกคือ ไคโตซานดัดแปรซึ่งเป็นตัวเคลือบอยู่ชั้นนอกของอนุภาค โดยไคโตซานที่
ดัดแปลง (Bi-QCS) ประกอบด้วยประจุบวก (Quat188) และโมเลกุลเป้าหมาย (ไบโอติน) เพื่อเพิ่มการดูด
ซึมของเซลล์และควบคุมการปลดปล่อยยา หลังจากนั้น 5-Fluorouracil (5-FU) ซึ่งเป็นสารต้านมะเร็งถูก
บรรจุลงใน BiQCS-AuNPs@collagen โดย Bi-QCS-AuNPs@collagen ได้รับการพิสูจน์เอกลักษณ์ด้วย
เทคนิคต่างๆ ซึ่งพบว่า ขนาดอนุภาคของ AuNPs@collagen เพิ่มขึ้นหลังจากเคลือบด้วย Bi-QCS จาก
30 นาโนเมตรเป็น 50 นาโนเมตรในขณะที่ศักยภาพของซีตาเปลี่ยนจากค่าลบ (ไม่เคลือบผิว) เป็นค่าบวก
(เคลือบด้วย Bi-QCS) การเคลือบ Bi-QCS บนพื้นผิวของ AuNPs @ collagen สามารถเพิ่มประสิทธิภาพ
ในบรรจุยา 87.46% ในขณะที่ AuNP @ collagen แสดงประสิทธิภาพในการบรรจุยาเพียง
64.67% นอกจากนี้ Bi-QCS-AuNPs@collagen ยังสามารถควบคุมการปลดปล่อยของยา ซึ่งที่ pH 5.4
แสดงอัตราการปลดปล่อยของยาที่สูงกว่า pH 7.4 หลังจาก 48 ชั่วโมง จากนั้นได้ทำการศึกษาฤทธิ์ทาง
ชีวภาพของ Bi-QCS-AuNPs@collagen พบว่ามีฤทธิ์ต้านการอักเสบและช่วยเพิ่มประสิทธิภาพในการ
ต้านมะเร็งของ 5-FU ที่สูงขึ้นอย่างมีนัยสำคัญ

สาขาวิชา   เคมี   ลายมือชื่อนิสิต ....
ปีการศึกษา   2563   ลายมือชื่อ อ.ที่ปรึกษาหลัก ....
                                          ลายมือชื่อ อ.ที่ปรึกษาร่วม ....

6172133423 : MAJOR CHEMISTRY

KEYWORD: Gold nanoparticle; coating; chitosan modification; anti-inflammatory; anti-cancer; 5-Fluorouracil

Naruthai Hongsa : DESIGN AND SYNTHESIS OF MODIFIED CHITOSAN/COLLAGEN COATED-GOLD NANOPARTICLES AS A CARRIER FOR ANTICANCER AND ANTIINFLAMMATORY AGENTS. Advisor: Prof. NONGNUJ MUANGSIN, Ph.D. Co-advisor: Kanokwan Sansanaphongpricha, Ph.D.

The proposes of this research are to improve the delivery efficiency of AuNPs. One of the problems with drug loading and drug degradation, the drug was loaded onto the surface of the gold particles, adheres to the outer of the surface, which was easy to decompose in the body. In this work, we have developed the coated AuNPs by modified chitosan (Bi-QCS), which the Biotin-Quat188-AuNPs@collagen (Bi-QCS-AuNPS@collagen) was designed as follow: (i) collagen was used as a reducing agent and a stabilizing agent in the AuNPs@collagen, while (ii) modified chitosan (positive charge polymer) was coated on the outer layer, which modified chitosan (Bi-QCS) was consists of a positive charge (Quat188) and a targeting molecule (biotin) to increase cellular uptake and control drug release. After that, 5-Fluorouracil (5-FU) as an anticancer agent was loaded into BiQCS-AuNPs@collagen. The Bi-QCS-AuNPs@collagen was characterized by many techniques. The particle size of AuNPs@collagen increased after coating with Bi-QCS from 30 nm to 50 nm, while the zeta potential change from a negative value (uncoated) to a positive value (coated with Bi-QCS). The coating of Bi-QCS on the surface of AuNPs@collagen can increase the loading efficiency was 87.46 %, while the AuNP@collagen shows a loading efficiency of only 64.67 %. In addition, Bi-QCS-AuNPs@collagen can control the drug release rate, which at pH 5.4 showed the drug release rate higher than pH 7.4 after 48 hours. The evaluation of the biological activity of Bi-QCS-AuNPs@collagen presented significantly higher anti-inflammatory activity and anticancer activity of 5-FU.

Field of Study:	Chemistry	Student's Signature	
Academic Year:	2020	Advisor's Signature	
		Co-advisor's Signature	

ACKNOWLEDGEMENTS

Naruthai Hongsa

TABLE OF CONTENTS

List of Tables

List of Figures

LIST OF ABBREVIATIONS AND SYMBOLS

^{1}H NMR	Proton nuclear magnetic resonance
FTIR	Fourier transformed infrared spectroscopy
TEM	Transmission electron microscope
UV-vis	UV-vis spectrophotometer
DLS	Dynamic light scattering
ICP-AES	Inductively coupled plasma atomic emission spectroscopy
v/v	Volume/volume
w/v	Weight/volume
mL	Milliliter
µL	Microliter
mmol	Millimole
g	Gram
%DQ	Degree of quaternization
ppm	Part per million
mM	Millimolar
µM	Micromolar
nm	Nanometer
h	Hour
min	Minute
mg	Milligram
°C	Celcius degress
A549	Lung cancer cell
FBS	Fetal bovine serum
RAW 264.7	Murine macrophage cells line
HeLa	Cervical cancer cell
MTT	3-(4,5-dimethylthiazol-2-yl)-2,5-diphenyltetrazolium bromide dye
LBL	Layer-by-Layer
AuNPs	Gold nanoparticles
IM	Imitanib
PEI	Poly-ethyleneimine
PSS	Poly-styrenesulfonate
5-FU	5-Fluorouracil

Bi	Biotin
HAuCl$_4$	Chloroauric acid
EDC	1-ethyl-3-(3-dimethylaminopropyl) carbodiimide
NHS	*N*-hydroxylsuccinimide
PBS	Phosphate buffered saline
DMSO	Dimethyl sulfoxide anhydrous
CF$_3$COOH	Trifluoroacetic acid
TMS	Tetramethylsilane
KBr	Potassium bromide
NaOH	Sodium hydroxide
A549	Lung cancer cell
FBS	Fetal bovine serum
RAW 264.7	Murine macrophage cells line
HeLa	Cervical cancer cell
LPS	Lipopolysaccharides
NO	Nitric oxide
Quat188	*N*-(3-chloro-2-hydroxypropyl) trimethylammonium chloride
QCS	*N*-(3-chloro-2-hydroxypropyl) trimethylammoniumchloride-chitosan
AuNPs@collagen	gold nanoparticles-collagen
Bi-QCS	Biotin- *N*-(3-chloro-2-hydroxypropyl) trimethylammoniumchloride-chitosan
Bi-QCS-AuNPS@collagen	Biotin- *N*-(3-chloro-2-hydroxypropyl)-trimethylammoniumchloride-chitosan-gold nanoparticle-collagen

CHAPTER I

INTRODUCTION

1.1 Research background

The drug delivery system (DDS) is the application of nanotechnology to improve the efficacy of drug carriers. This system used to enhance the treatment of patients such as cancer inhibition, anti-inflammatory, and reduce therapeutic side effects that arise from the use of high-dose drugs [1]. In recent years, nanoparticles have been developed for drug carriers because of the suitable properties such as able to control the release of the drug and can deliver target drug to specific surfaces of target cells [2].

Gold nanoparticles (AuNPs) are one of the most popular drug carriers for the drug delivery system. Due to the unique properties consist of low cytotoxicity, tunable size, biocompatibility [3]. Moreover, the highly tunable and multivalent surface structures of AuNPs affect a variety of functionalization. The ability to tailor the surface has made AuNPs effective in both active and passive targeting [4]. Nowadays, there have a variety of AuNPs synthesis methods, the most common method is a chemical method. Among the chemical synthesis category, two methods that the most widely known and used are the Turchevich-Frens and Brust-Schriffin methods [5, 6]. However, this technique has several disadvantages such as reproducibility, toxic chemical, and difficult steps. Due to these drawbacks, the green synthesis methods (biopolymer) are attractive because of the less toxicity, biocompatibility, controller of the drug release, and uncomplicated synthesis method. For example, used bacteria, fungi, plant extracts proteins and amino acids in collaboration with outside energy sources such as ultrasound, light, and microwave to synthesis AuNPs [7, 8]. Even though the green methods produce less toxic nanoparticles, there still needs more optimization of drug loading efficiency on AuNPs surface and the stability [9]. In the same way, improving the surface of gold nanoparticles as the type of monolayer or multilayer has been applied to improve stability and efficiency of drug loading [10]. Currently, coating of nanoparticles by layer-by-layer (LBL) technology is an attractive topic with many

potential applications in drug delivery [11]. The layer-by-layer coating on the surface can improve the stability, the release rate of the drug and enhance the skin permeability of sodium hyaluronate chitosan [12]. The layer-by-layer coating of AuNPs also enabled imitanib (IM) loading, prepared using the poly-ethyleneimine (PEI) and poly-styrenesulfonate (PSS) polymers proved to successfully increase drug loading capacity on the surface of gold nanoparticles via electrostatic interactions [13]. Therefore, the role of the layer-by-layer coating is to control the release rates of the drug and to prevent degradation of the drug enhancing its stability which is a result of the electrostatic interactions [14, 15]. According to the Derjaguin-Landau-Verwey-Overbeek (DLVO) theory, a colloidal solution requires repulsive forces such as electrostatic or steric stabilization to prevent aggregation from occurring [16].

An option to stabilize nanoparticles would be a polymer or a protein that prevents nanoparticles from aggregation by adsorbing on their surface [17]. Moreover, protein coronas on the surface of the nanoparticles can provide different functional groups for surface conjugations of other molecules such as dyes, antibodies, or drugs [18]. At present, collagen is one of the most important and abundant structural proteins in the extracellular matrix which has been widely used in biomaterial applications and a versatile coating [19]. Because it combines all mandatory characteristics for biological applications namely, biocompatibility, accessibility, and safety [20]. Moreover, collagen also contains amino acids which have a reducing agent property for the synthesis of gold nanoparticles. Amino acids present a negative charge around the gold nanoparticle surface. These charges can prevent particle aggregation and also create electrostatic interactions with positively charged molecules (such as chitosan, cyclodextrin, gelatin, and cellulose) generating a polyelectrolyte complex.

Chitosan has been widely used as a particle-forming polymer and a surface coating. Several *in vitro* and *in vivo* studies have shown modifying the surface of those types of nanocarriers by coating them with chitosan. This technique can confirm many advantages consist of improve physicochemical stability, control drug release, promote tissue penetration, modulate cell interactions (cellular uptake and toxicity), and

enhance anti-inflammatory activity [21]. Stimuli response is an important property that affects the ability of systems to deliver drugs effectively. Drug release could be triggered by physical or chemical stimuli such as pH, ionic strength, temperature, magnetic, and biological molecules. The chitosan exhibits a pH-sensitive behavior due to the large quantities of amino groups on its chains [22], which can undergo volume phase transitions from swollen to collapsed states depending on the pH of the solution. This advantage of chitosan is critical to control the release of the drug from the nanocarrier to the target area [23].

In order to increase the drug's ability to act, the nanocarrier must control the release of the drug at the target cells and the surface of the nanocarrier can be decorated with specific target molecules (e.g., biotin, folate, or cRGD tripeptide) to increase specificity with the target cells. Among all targeting molecules, biotin plays an important role related to the expression of biotin receptors on the surface of tumoral cells especially, cervical, ovarian, and lung cancer cells. Biotin is into the cancer cells through receptor-mediated endocytosis mechanisms. Several researchers have shown that the biotin-conjugated polymeric carriers can stimulate a higher uptake of their corresponding cargoes by the tumor cells [24]. Such improvements can enhance the efficacy of drugs and reducing the side effects to other cells [25].

5-Fluorouracil (5-FU) has been used for the treatment of various cancers such as colorectal, lung, gastrointestinal, and skin cancer. It is a pyrimidine-analog antineoplastic antimetabolite that interferes in DNA synthesis by blocking deoxyuridylic acid conversion into thymidylic acid through thymidylate synthase [26]. Similarly to other drugs used for chemotherapy, it also affects the growth of normal cells and often causes side effects. Therefore, a ligand targeting carrier is necessary for 5-FU delivery to reduce off-targeting adverse reactions [27, 28]. Therefore, a ligand targeting carrier is necessary for 5-FU delivery to reduce off-targeting adverse reactions.

1.2 Scope of Research.

In this study, we reported herein polyelectrolyte coated AuNPs (Bi-QCS-AuNPS@collagen) with greater 5-FU loading compared to those traditional gold

nanoparticles. The Bi-QCS-AuNPS@collagen was designed as follow: (i) collagen, a negative charge polymer, was used as a reducing agent and a stabilizing agent in the AuNPs@collagen, while (ii) modified chitosan, a positive charge polymer, was coated in the outer layer, containing (iii) biotin, a targeting molecule to increase cellular uptake and control drug release. Bi-QCS-AuNPS@collagen and 5-FU-loaded Bi-QCS-AuNPS@collagen were characterized and evaluated for their safety profile, anti-inflammation, cancer suppression in vitro as shown in Fig 1. The layer-by-layer coating of the nanoparticles was designed to enhance 5-FU loading due to strong electrostatic interaction and H-bonding. It is also highlighting that Bi-QCS-AuNPS@collagen is a pH sensitive nanoparticle, which can prevent premature release in a normal physiological pH but rapidly release the drug in an acidic condition in tumor microenvironment. Therefore, Bi-QCS-AuNPS@collagen may have a potential for further studies *in vivo* and in a clinical setting.
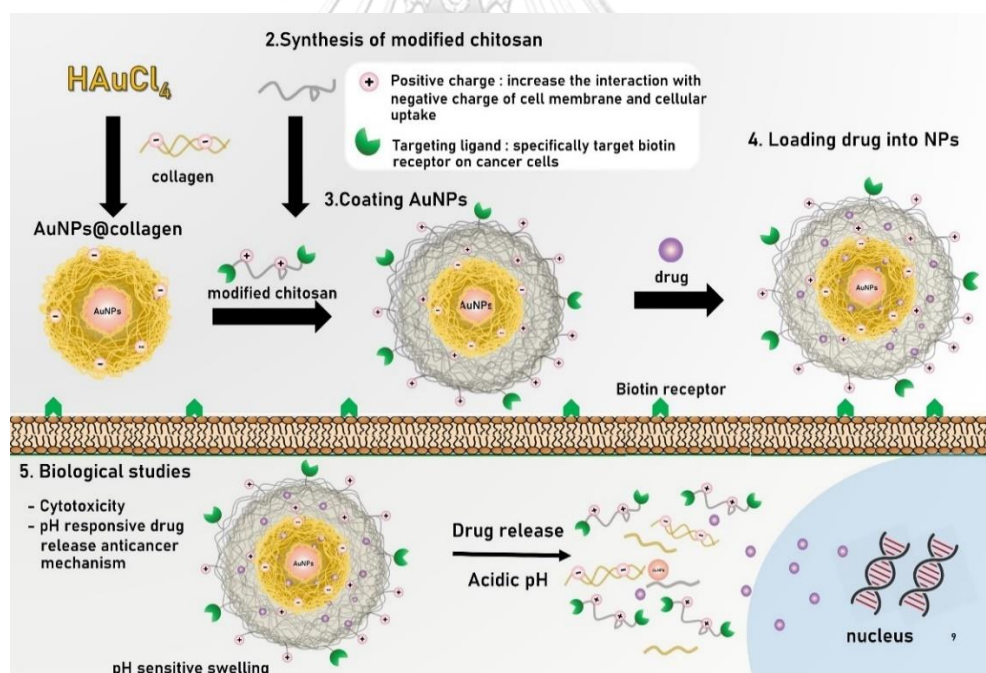
Figure 1 Scope of this research

1.3 Research objectives

The purposes of this research are to develop the coated AuNPs by modified chitosan(Bi-QCS), which the Biotin-Quat188-AuNPs@collagen (Bi-QCS-AuNPS@collagen)

was designed as follow: (i) collagen was used as a reducing agent and a stabilizing agent in the AuNPs@collagen, while (ii) modified chitosan (positive charge polymer) was coated on the outer layer, which modified chitosan (Bi-QCS) was consists of a positive charge (Quat188) and a targeting molecule (biotin) to increase cellular uptake and control drug release. After that, 5-Fluorouracil (5-FU) as an anticancer agent was loaded into BiQCS-AuNPs@collagen for testing anti-inflammatory activity by nitric oxide assay and anti-cancer activity by MTT assay. The objectives of this research were described as follow;

1. To improve the delivery efficiency of AuNPs

2. To improve the surface of gold nanoparticles to be more effective for drug loading

3. To design the surface of gold particles to prevent drug degradation and control of drug release in conditions where target cells grow
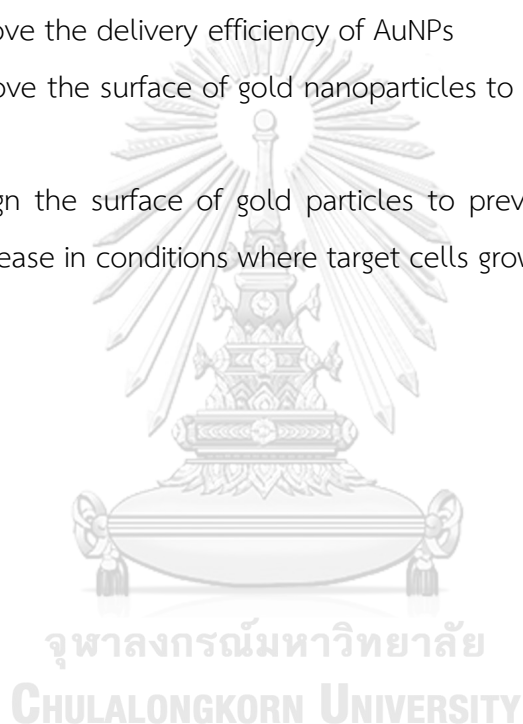
CHAPTER II
LITERATURE REVIEW

2.1 Drug delivery system

Currently the procedure for treating patients with health problems, there have many different types of treatment. The primary treatment method is medication to treat symptoms that occur, but the drug treatment is low efficacy and has side effects in some patients. Because the drugs have reacted with normal cells, cannot specific to target cells, and drugs have been destroyed before reach the target cells, which resulted in a decrease in the effectiveness of treatment. For this reason, it has led to a study of the delivery of drugs into target cells using the application of nanotechnology.

Drug delivery system (DDS) is the application of nanotechnology to improve drug efficacy. DDS is a process of preparing formula or device that enables the introduction of a therapeutic substance in the body, improves efficacy and safety by controlling the rate, time, and place of drug release in the body. This system used to enhance the treatment of patients such as anti-cancer, anti-inflammatory, and reduce therapeutic side effects that arise from the use of high-dose drugs [1]. In recent years, nanoparticles have been developed for drug carriers because of the suitable properties such as able to control the release of the drug and can deliver the drug to specific surfaces of target cells [2]. The criteria for selecting the nanoparticle are based on the physical and chemical features of drugs. Afterward, nanotechnology has developed drug carriers that combined with bioactive natural compounds to enhance bioactivities for treating cancer and many other diseases.

DDS created many types of nanocarriers depend on the composition of the materials. The nanocarriers were divided into organic, inorganic, and composite materials as show in Fig 2 [29].
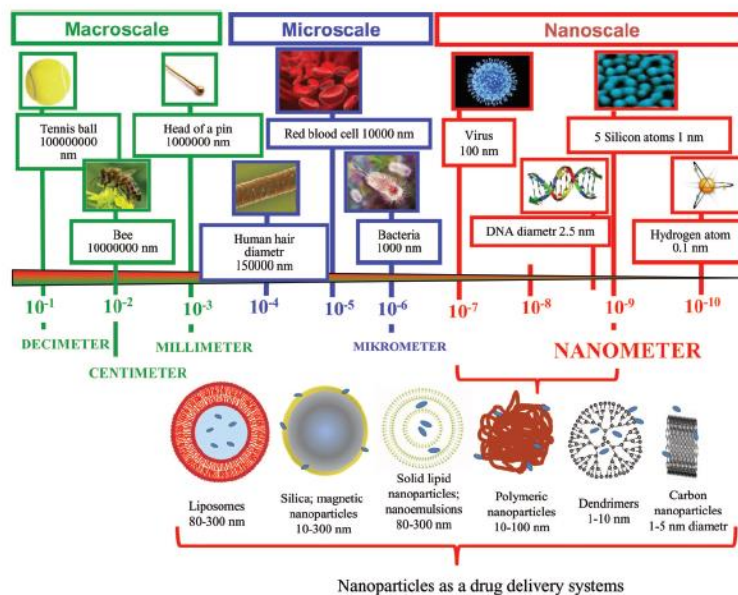
Figure 2 Nanoparticle drug delivery systems with relation to other [30]

2.2 Nanocarriers

The success of free transport greatly depends on the design of the drug carrier. Given their small nano-size (at least in one dimension), nanoparticles (NPs) make ideal drug carriers because they can diffuse across a variety of barriers, such as capillary walls or membrane pores, between cells forming protective layers or directly into diseased tissue that leading to local drug accumulation [31]. Drug carrier divides into many types as shown in Fig 3.

2.2.1 Lipids

Liposomes, which consist of a lipid bilayer surface enclosing an aqueous core, were the first drug carriers used for targeted drug delivery [32]. Due to their structure of hydrophilic heads stabilized by surfactants and multiple hydrophobic tails, they are able to encapsulate both hydrophilic and hydrophobic drugs [33].

The liposomes have many properties such as small nano-size, easy surface manipulation, biocompatibility, biodegradability, and their multi-route options for injection that make them attractive carriers. Thus, they have been approved for multiple clinical trials. Apart from their advantages, they have the major limitation of

drug carriers consist of premature and uncontrolled drug release due to their leaky structure [34].

2.2.2 Polymers

Polymer drug carriers have been used in the form of nanoparticles, micelles, dendrimers, hydrogels, and natural polymers such as PLGA (poly-D, L-lactide co-glycolide) and PLA (polylactide). Nano-size micelles are usually spherical in shape and either be solid or hollow for loading the drug. On the other hand, dendrimers are macromolecules that branch out into tree-like forms from a central core. The usage of dendrimers is of interest since they are monodisperse, highly symmetric, water-soluble, and able to encapsulate hydrophobic nano drugs [35, 36]. The loading drugs onto these carriers occurred covalent attachment adsorption to the surface or entrapment in the polymer matrix [37]. In addition, they have characteristics such as biocompatibility, biodegradability, and water solubility that make polymers were one of the most popular drug carriers [36]. However, some issues that remain to be addressed were the heterogeneity of manufactured polymer nanoparticles and the possible cytotoxic effects resulting from non-targeted cellular uptake [38].

2.2.3 Carbons

Carbon-based particles are usually in the form of carbon nanotubes (CNTs) just 0.3 nm thick, benzene ring shape, which distinctly different from the carbon forms of graphite and diamonds. Moreover, the structure belongs to the family of fullerenes. Due to their ultrahigh surface area relative to the volume, biomolecules can be attached to the CNT walls and tips and can also be loaded inside CNTs. Despite these advantages, their major limitation is their possible cytotoxicity due to the metal catalyst and amorphous carbon contaminants which are often present and difficult to remove [39].

2.2.4 Metals

The metal was used to nanoparticles include nano-shells (metallic covered silica particles), gold nano-cages (hollow, porous metallic particles), and gold nanoparticles. They are attractive carriers because of their very small (<50 nm), stable shapes, electrically charged, high surface reactivity, and biocompatibility. These NPs are often used for imaging or hypothermia-based therapies in which the particles absorb light and emit heat to destroy tumor cells. Magnetic nanoparticles (MNPs) are also useful metal-based NPs because they can be employed to enhance contrast agents in magnetic resonance imaging (MRI), or they can function as drug carriers that can be directed towards tumors via a locally applied magnetic field [36]. Often, magnetic iron oxide particles (Fe_3O_4 or Fe_2O_3), with a synthetic or a natural polymer surface coating to help avoid particle agglomeration, are used in this application. As with the other drug carriers, metal-based NPs can also be modified to targeting ligands of drugs, which can be released from the drug carriers by local changes in the physiological conditions (e.g. temperature and/or pH) near/at the target site [40].

2.2.5 Ceramics

Ceramic NPs, often in the form of mesoporous silica NPs, are novel nanocarriers that are porous and less than 50 nm in mean diameter. They are desirable for transporting drugs which are susceptible to changes in pH since they are unaffected by this condition. Furthermore, they have an increased surface area for incorporating drugs, with their multitude of pores, and simultaneously their surfaces can be modified to include connective ligands. However, they showed side effects on normal cells and not biodegradable [41].

2.2.6 Viruses

Viruses have also been proposed as potential drug carrier candidates due to the innate attraction of certain viruses to specific overexpressed receptors on tumor cells. Through genetic alteration, infection is not only avoided but viruses can also be designed to target tumor cells. For example, hepatitis B core particles have been

demonstrated as potential delivery agents to liver cells. However, a major limitation of using viruses as drug carriers was their potential for developing severe complications [42].
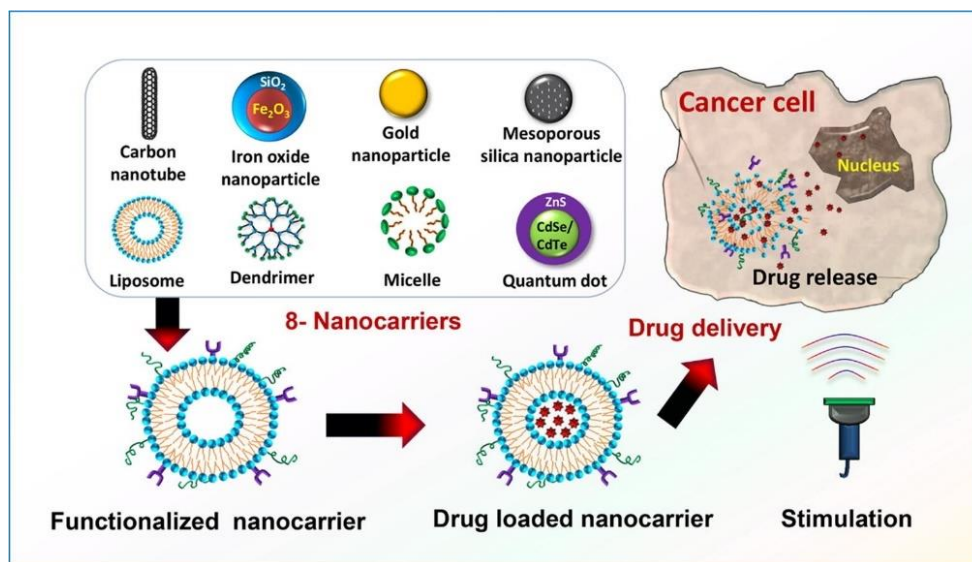
Figure 3 Type of Nanocarrier [43]

2.3 Gold nanoparticles (AuNPs)

Gold nanoparticles provide an outstanding material for study due to they are one of the most stable, non-toxic, easy to synthesize nanoparticles and exhibit various fascinating properties like the assembly of various types and quantum size effect. The optical behavior of gold nanoparticles is dependent on their surface plasmon resonance (SPR), located in a wide region ranging from visible to the infrared region of the spectrum, which is determined by the collective oscillation of conducting electrons. The range of the spectrum depends on various features of gold nanoparticles, including size and shape [44]. Methods have been developed to synthesize these materials reproducibly, which can further be modified using countless chemical functional groups as shown in Fig 4. Many new sensitive and specific assays are based on gold nanoconjugates. Moreover, the shape of particles can affect cell permeability where gold nanoparticles can tunable size and spherical shape. Additionally, previously reported presents elliptical or tubular particles to take longer

to endocytose than spheres. Gold nanoparticles have emerged as an excellent candidate for the application in the delivery of various molecules to the target site, these molecules range from small drug molecules to large biomolecules like DNA, RNA, and proteins. Some drugs molecules do not require modification of a monolayer of gold nanoparticles for their delivery and can be directly conjugated with gold nanoparticles through physical absorption and ionic or covalent bonding [45]. Thus, gold nanoparticles are an interesting drug carrier due to their properties.
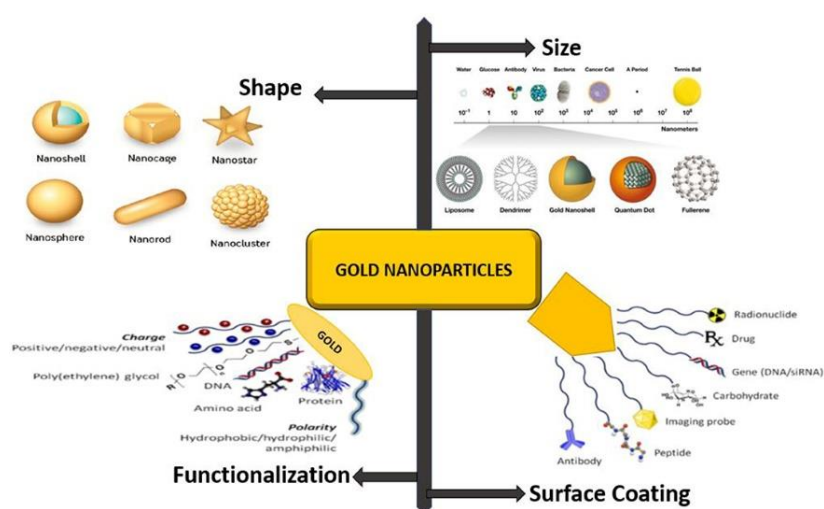
Figure 4 Spherical to Nanostar morphology of AuNPs, Functionalization by Antibody, Carbohydrate, DNA/RNA, peptide, loading with drugs, and used for probing Image [46].

2.4 Synthesis of AuNPs

For the synthesis of AuNPs, there are two basic strategies that are used consist of "Top-Down" and "Bottom-Up" approaches. The top-down approach involves the synthesis of AuNPs starting from bulk material and cracking it into nanoparticles using different methods. In contrast, the bottom-up approach synthesized nanoparticles starting from the atomic level. Fig 5 shows the basic steps that are involved in the top-down and bottom-up approaches. In the first stage the gold precursor, which is usually an aqueous gold salt solution, is reduced to gold nanoparticles using a specific reducing agent like citrate. In the second stage the stabilization of gold nanoparticles is done

by a specific capping agent. The capping agents hinder the agglomeration of metallic nanoparticles as shown in Fig 5.

Synthesis methods involve the top-down approach include laser ablation, ion sputtering, ultraviolet–visible (UV), infrared (IR), and aerosol technology, whereas the reduction of Au^{3+} to Au^0 is the bottom-up approach [47].
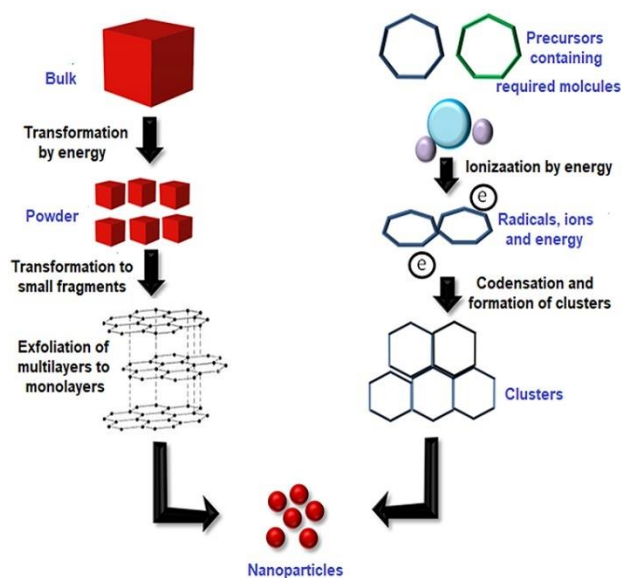
Figure 5 Top-down and bottom-up approaches for the synthesis of NPs [47].

2.4.1 Chemical Synthesis

2.4.1.1 Turkevich Method

One of the most common techniques was used to synthesis of spherical AuNPs. AuNPs were prepared using this method which has the size in the range of 1–2 nm. The basic principle of this technique involves the reduction of gold ions (Au^{3+}) to produce gold atoms (Au^0) by using some reducing agents like amino acids, ascorbic acid, UV light, or citrate as shown in Fig 6A. Stabilization of AuNPs is carried out by using different capping or stabilizing agents [48]. Turkevich method is a fairly uncomplicated and reproducible procedure for the formulation of spherical particles with a size range of 10–30 nm. However, the size of particles increases above 30 nm,

they become less spherical in shape with broader size distribution. Moreover, this reaction produces a low yield and the use of only water as a solvent [49].

2.4.1.2 The Brust Method

This method was first reported in 1994 and involves a two-phase reaction to synthesize AuNPs with a size range of 1.5–5.2 nm by using organic solvents. The method encompasses the use of a phase transfer such as tetraoctylammonium bromide to carry out transferring of gold salt to organic solvent from its aqueous solution (e.g. toluene). Then, the gold was reduced by using a reducing agent such as sodium borohydride along with an alkanethiol. The alkanethiol carries out the stabilization of AuNPs as shown in Fig 6B. As a result of this reaction, the color changes from orange to brown [50]. The Brust method is an easy strategy for the formulation of thermal and air-stable AuNPs that having controlled size and less dispersity. One possible limitation of the Brust method is the synthesis of AuNPs which are less dispersed and used organic solvents immiscible with water.
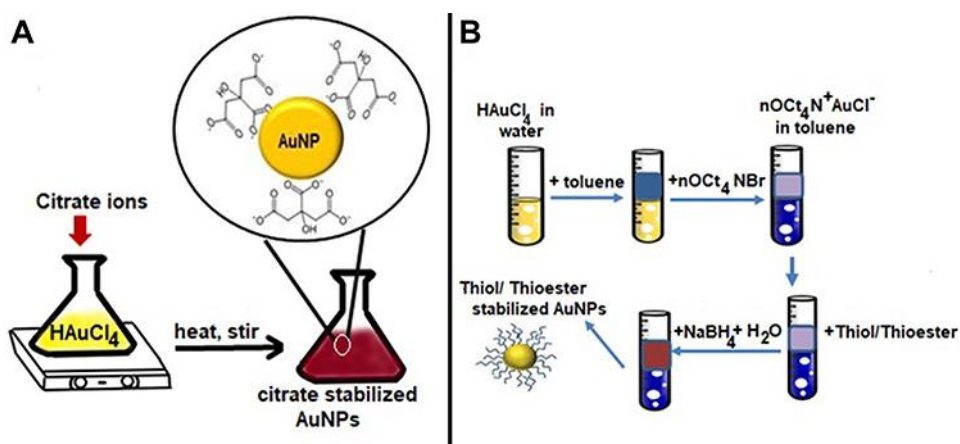
Figure 6 (A) Turkevich method for the synthesis of AuNPs. (B) Series of steps involved in the Burst method for the synthesis of AuNPs [47].

2.4.2 Biological Synthesis

Recently, efforts have been made for the biological synthesis of AuNPs, which is a clean, dependable, and bio-friendly, alternative to harsh chemicals used in chemical synthesis reactions. The biological resources were used in the synthesis of nanoparticles range from simple bacterial cells to complex eukaryotes. Interestingly, the capability of organisms for the synthesis of metal nanoparticles has given rise to a new thrilling approach toward the development of these biological nano-factories. A plethora of organisms have been reported to carry out the successful synthesis of AuNPs, ranging from bacteria to plants, algae, and fungi.

Molecules synthesized by living organisms to speed up their biological processes of the body are known as biomolecules such as amino acids, nucleic acids, carbohydrates, and lipids. Previous studies have reported the synthesis of gold nanoparticles using chitosan which does not only act as a reducing agent but also as a stabilizing agent during the synthesis reaction. Apart from that, starch was another polysaccharide used for the synthesis of AuNPs. In an alkaline environment, starch could be degraded into short chains consist of carboxyl groups and the –OH group of carboxylic acid which could reduce Au^{3+} ions to gold nanoparticles. The biological method could decrease the toxicity of the chemicals used for the synthesis AuNPs [51].

2.4.2.1 Protein

Amino acid is a subunit of protein that can be used to carry out the synthesis reaction of AuNPs. The previous studies reported the preparation and characterization of coated GNPs using amino acid as a reduction agent and also as a surface modifier. The tyrosine amino acid was successfully synthesis the gold nanoparticles [52]. It had been verified that tyrosine plays a basic role in the reduction of Au^{3+} to Au^{0}. The biocompatibility assessment of AuNPs both in vitro and in vivo had recently reported that amino acid-AuNPs were friendly to the natural system and as non-toxic material for various biological applications as shown in Fig 7.

Ramezani *et al.* investigated the adsorption of amino acids on AuNPs via molecular dynamics simulations and offered the following observations [53]: the amino acids containing hydroxyl groups in their side chains (tyrosine, threonine, and serine) were adsorbed on the surface through Au–OH interactions. Alanine, valine, isoleucine, and leucine, having linear side chains, were adsorbed on the AuNPs surface by their methyl groups. Glycine was adsorbed through its carboxyl group. Histidine, arginine, asparagine, glutamine, and lysine that adsorb on the AuNPs surface were enabled by the amino groups in their side chains. The interaction of AuNPs with the negatively charged amino acids (such as aspartic acid and glutamine) occurred through the side-chain carboxyl groups. The aromatic ring of phenylalanine participated in the adsorption on the AuNPs surface. Cystine, cysteine, and methionine were adsorbed on the AuNPs through their sulfur atoms. Proline interacted through its amine (Au–N) and carboxylic groups (Au–O and Au···H–O) [54]. This result offered significant opportunities for developing nanoparticle-based therapeutics against diseases related to protein aggregation. Synthesis of AuNPs using protein-based material was a facile and uncomplicated process. Various attributes of AuNPs such as shape and size can be regulated by controlling the reaction parameters. Additionally, the reaction process is fast and economical.
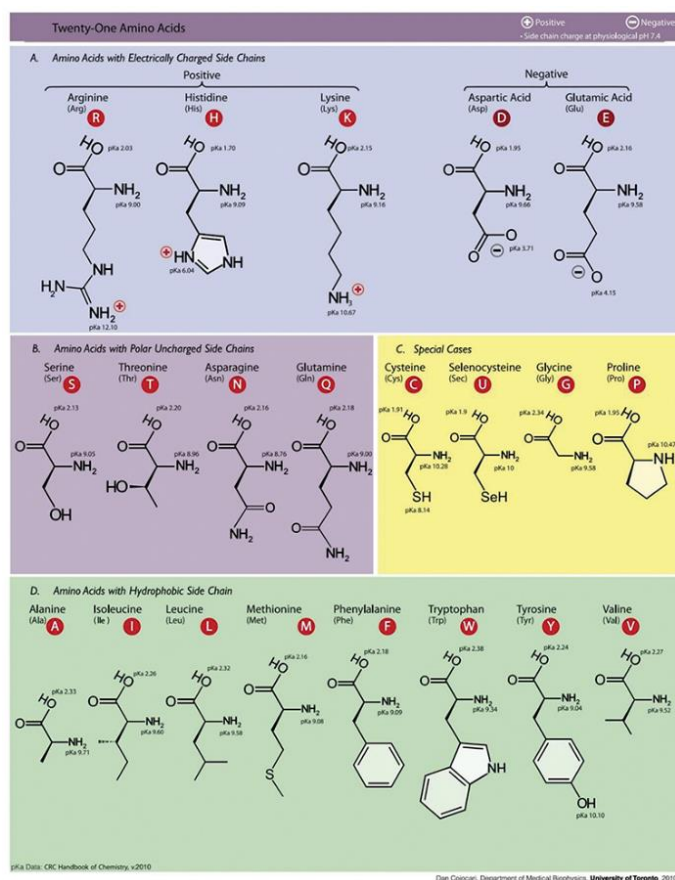
Figure 7 Amino acid as a reducing agent for synthesis gold Nanoparticles [55]

2.5 Functionalization of AuNPs

AuNPs can be functionalized in a number of ways which generate the possibilities for a variety of approaches for their use in designing drug delivery systems (DDS) as shown in Fig 8. When non-covalent interactions are used for the loading of drugs on nanoparticles, no specific bond cleavage is required to carry out the efficient drug release and only alterations in native physical forces are needed. Similarly, AuNPs can be covalently bonded to the drug through cleavable bonds forming a prodrug that can be delivered to the cell liberating the drug from AuNPs using either external or internal stimuli. However, the modification of the monolayer of AuNPs is very important for the extracellular or intracellular discharge mechanisms.
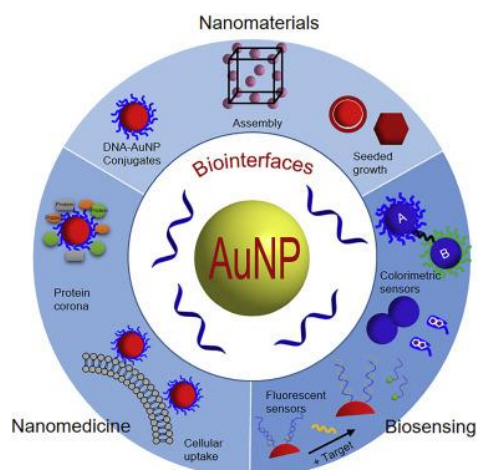
Figure 8 The surface of the gold nanoparticle can be developed to several functions [56].

2.6 The Layer-by-Layer coating on the surface particles (LBL coating)

Polyelectrolytes (PEs) were polymers of repeating units that contain an ionizable group. These charged polymers could be used to coat surfaces particles in a number of ways including covalent attachment, hydrogen bonding, and electrostatic interactions between layers [57].

Nowadays, coating of nanoparticles by layer-by-layer (LBL) technology is an attractive topic with many potential applications in drug delivery [11]. The hyaluronate chitosan multilayered coated liposomes could improve the stability, control the release rate of the drug, and enhance skin permeability of quercetin [12]. The layer-by-layer coating of AuNPs also enabled imitanib (IM) loading, prepared using the poly-ethyleneimine (PEI) and poly-styrenesulfonate (PSS) polymers proved to successfully increase drug loading capacity on the surface of gold nanoparticles via electrostatic interactions [13].

Layer-by-Layer coatings with polyelectrolyte have distinct advantages over other surface modification methods, specifically the ease of assembly on a wide range of substrates. The deposition of PEs onto NP surfaces simply relies on electrostatic interactions that govern the layer-by-layer attachment process of positive charge and negative charge of the molecule as shown in Fig 9 [57].

The coating methods have to be optimized, especially when depositing PEs onto NPs, as the colloidal stability of the system can be easily affected. According to the Derjaguin-Landau-Verwey-Overbeek (DLVO) theory, a colloidal solution requires repulsive forces such as electrostatic repulsion or steric stabilization to prevent aggregation [58]. The colloidal stability in PE-coated NPs is extremely important for biomedical applications because the aggregation can alter their in vitro behavior such as NP uptake and cytotoxicity [59]. Therefore, the role of the layer-by-layer coating is to control the release rates of the drug, prevent degradation of the drug, and enhancing its stability which is a result of the electrostatic interactions [14, 15].
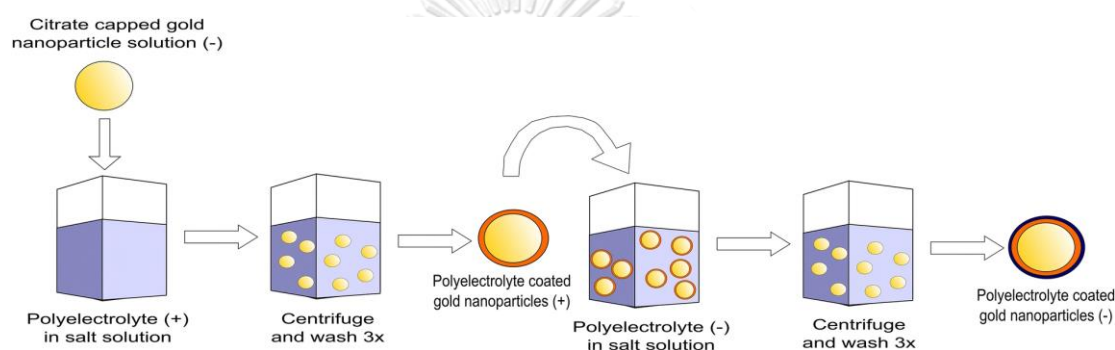
Figure 9 Method for self-assembly of polyelectrolyte-coated gold nanoparticles using the LbL method [60].

2.7 pH-Mediated Drug Release

One of the most appropriate conditions for the drug release at the site of the target over the surrounding tissues is pH. The acidic surrounding with the pH ranges from 5.7–7.8 is present in human cancer cells or inside the cell organelles including endosomes and vesicles. These specific pH conditions lead to the cleavage of acid sensitive bonds and charge switching due to protonation and morphological alterations of carriers. For example, the acidic conditions (pH 5.0) in lysosomes or endosomes or both can cause the cleavage of the hydrazone bond which is an acid-sensitive bond. This property of hydrazone bond has widely been used in the preparation of pH-responsive supramolecular fabrications for intracellular drug release as shown in Fig 10.

Chen *et al.* prepared dual-stimuli-responsive microcapsules with drug loading and controlled release behaviors [87]. In their study, pH-sensitive polymer particles (pNIPAM particles) were synthesized and loaded with Nile Red (NR) and oil-soluble fluorescent green (OG). At low pH conditions, the electrostatic repulsion of the positively charged polymer chains in the microcapsule shell caused the microcapsule shell to swell and release the OG, but the NR remained encapsulated inside the microcapsules. Therefore, the pH stimulus only triggered the release of OG molecules but had no influence on the NR molecules inside the particles. When the microcapsules were exposed to increasing temperatures, the NR molecules inside the particles were released because the microcapsules collapsed, but the OG molecules were unaffected [61].

In addition, a study had also reported the AuNPs modified with methyl thioglycolate (MTG) and thiolated methoxy polyethylene glycol (HS-mPEG) with a molar ratio of 1:1. When doxorubicin (DOX) was conjugated with MTG through a hydrazine bond, DOX-AuNPs conjugates showed higher pH-sensitive drug release at pH 5.3 compared to pH 7 (normal pH).
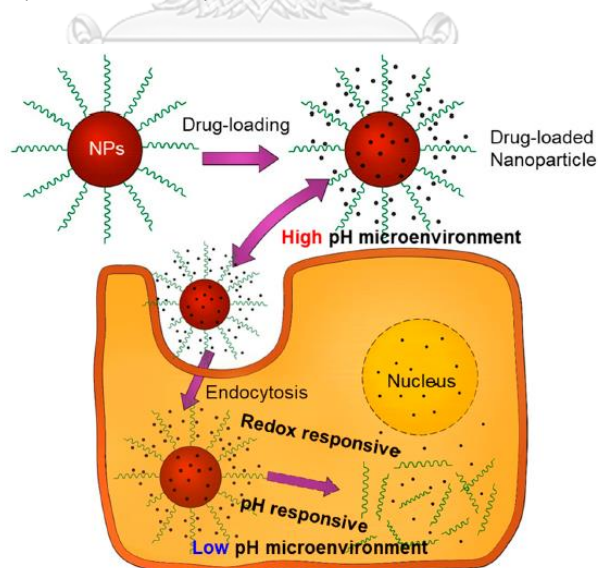
Figure 10 pH/redox potential dual-response-mediated drug release for tumor treatment [62].

2.8. Receptor-mediated endocytosis

Nanoparticles (NPs) are exogenous synthetic structures with nanoscale dimensions, which have raised enormous interest toward biological applications. Owing to their different size molecules, a way of the cellular uptake of NPs is necessarily different. For example, most of the molecules are unable to be internalized in cells by themselves (vide supra), NPs are incorporated into the cell via different endocytosis pathways. Additionally, the efficient uptake of engineered NPs have been proposed to improve the cellular permeability [63].

In the endocytosis process, the particles are first attached to the cell membrane through specific or nonspecific interactions. Then, are wrapped by the cell membrane to form membrane-bounded vesicles. The particles can enter cells by several different endocytic pathways such as phagocytosis, clathrin-mediated endocytosis, caveolae-mediated endocytosis, macropinocytosis, clathrin- and caveolin-independent endocytosis [64].

Phagocytosis is conducted primarily by specialized cells, including macrophages, monocytes, and neutrophils, which can clear out large particles in the blood such as pathogens and debris of dead cells. In contrast, pinocytosis can operate in all mammalian cells. Clathrin-mediated, caveolin-mediated, macropinocytosis, clathrin- and caveolin-independent endocytosis are four major processes of pinocytosis involving different types of receptor–ligand interactions, which are mainly dependent on particle size and surface chemistry as shown in Fig 11. Afterward, the particles can be transported to different cellular organelles such as cytoplasm, mitochondria, golgi complex, and even the nucleus [65]. Decuzzi and Ferrari proposed a similar theoretical approach that the contribution of nonspecific interactions (such as van der Waals and electrostatic forces) is as important as the specific receptor-ligand interaction [66].
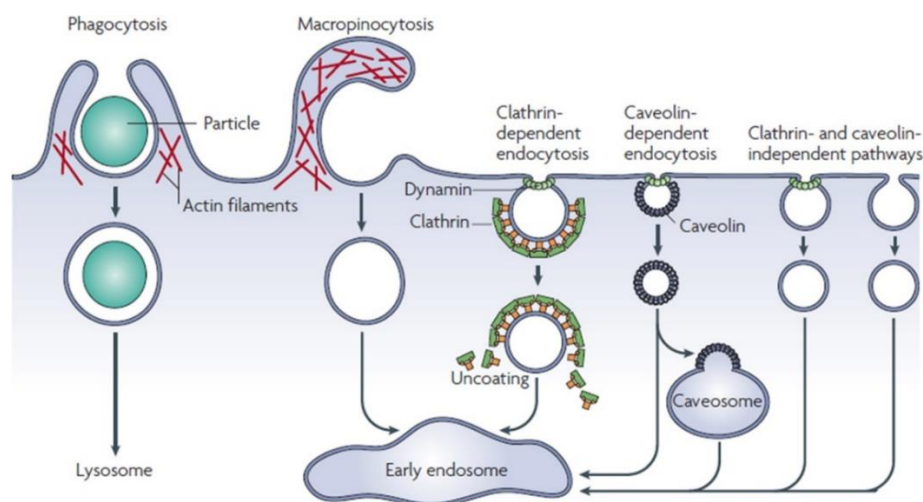
Figure 11 Schematic representation of the endocytic pathways used by cells to internalize molecules. Reproduced with permission from [63].

Receptor-mediated tumor targeting has received considerable attention in the field of anticancer therapeutics due to their specific action. Targeting the receptors, overexpressed in cancers, has opened new opportunities for intracellular targeting of drugs and delivery systems that are conjugated with targeting moieties, that is the ligands. This receptor-mediated targeting of anticancer drugs, especially using nano-sized carrier systems, protected them from the degrading body environment and improves their pharmacokinetic properties by extending their circulation time within the body as shown in Fig 12. Moreover, it also helps to overcome the systemic toxicity and adverse effects that arise due to the nonselective nature of most of the current anticancer therapeutic agents [67]. Additionally, the particle's surface charge can also affect cellular uptake, with positively charged particles being more readily endocytosed. Since conflicting characteristics are desirable in the different stages of targeting, it is suggested that ideal drug carriers should be able to dynamically alter their size, shape, or surface properties in vivo. Summarizes the influence of these characteristics, and the remainder of this section reviewed some of the current nano drug carrier designs [68].
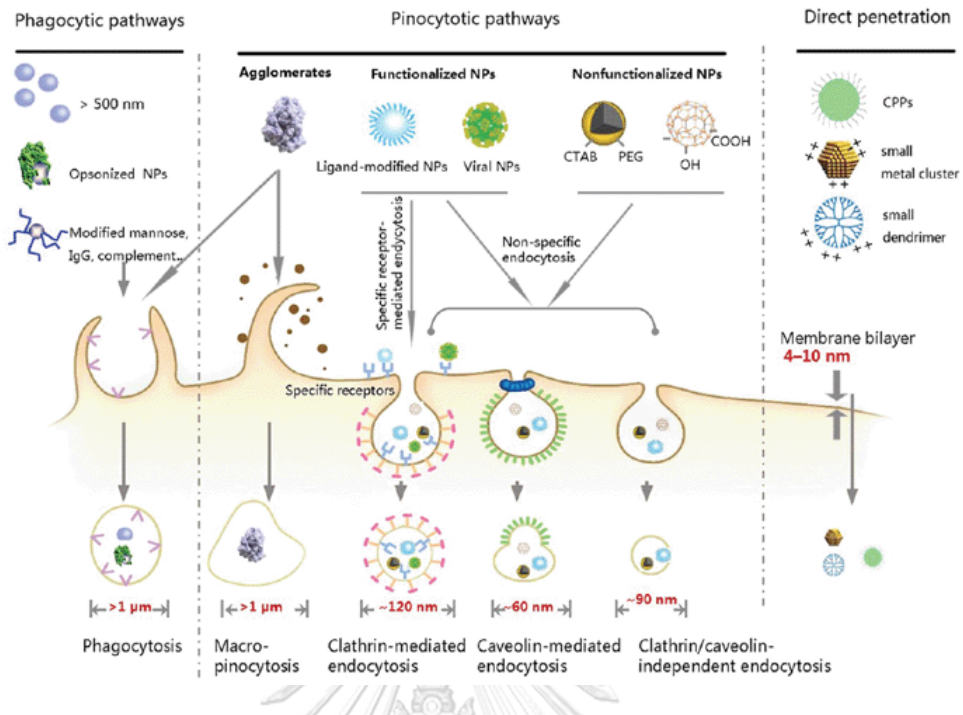
Figure 12 The cellular uptake of particles is dominated by the natural size rules and gatekeepers within a mammalian cell [69].

CHAPTER III

EXPERIMENT

3.1 Analytical Instrument

3.1.1 Transmission electron microscopy (TEM)

TEM was used to analyze the size and shape of the sample. The sample solution for analysis with TEM was prepared by dropping the dilute samples onto copper grids followed by dried in desiccators overnight. The micrographs were obtained on a transmission electron microscopy (HT-1400) operated at 80 kV.

3.1.2 Ultraviolet–visible spectroscopy (UV-vis)

The absorption of sample was analyzed by UV-vis spectrophotometer (Agilent 8453). The UV-vis spectra were recorded from 200 to 800 nm.

3.1.3 Fourier transformed infrared spectroscopy (FTIR)

The sample were analyzed by Nicolet iS50 FT-IR (US) in the region from 4000 cm^{-1} to 500 cm^{-1} in transmittance mode. The solid sample were prepared by pressing sample with potassium bromide (KBr) before analyzed with FTIR.

3.1.4 Inductively coupled plasma atomic emission spectroscopy (ICP-AES)

The concentration of Au was determined by Inductively coupled plasma atomic emission spectroscopy (ICP-AES) analysis. The samples were digested in aqua regia, HCl: Nitric acid (3:1), and diluted in milli-Q water.

3.1.5 Zetasizer

The particle size of the sample was measured using a dynamic light scattering (DLS) method with a particle size analyzer at 25 °C. Moreover, the surface charge of prepared sample was measured with a zeta potential value by electrophoretic light

scattering using a zetasizer. The samples for analysis with DLS and zetasizer were prepared by diluted with DI water (1:10 (v/v)).

3.1.6 Proton nuclear magnetic resonance (^{1}H NMR)

^{1}H NMR Spectra were at 500 MHz recorded on JEOL NMR spectrometer. ^{1}H NMR chemical shifts in chemical shifts in parts per million (ppm) were referenced relative to tetramethylsilane (TMS). The ^{1}H NMR data were processed with the MestRenova software.

3.2 Materials

Chitosan (average Mw of 500 kDa, degree of deacetylation = 85%) was provided by Seafresh Chitosan Lab (Thailand). Type I collagen (average Mw of ~900 kDa) was purchased from Chemipan Corporation (Thailand). Chloroauric acid (HAuCl4), 3-(4,5-dimethylthiazol-2-yl)-2,5-diphenyltetrazolium bromide dye (MTT), 1-ethyl-3-(3-dimethylaminopropyl)carbodiimide (EDC), Griess reagent, N-hydroxylsuccinimide (NHS) were obtained from Sigma-Aldrich (USA). Biotin, 5-Fluorouracil (5-FU) and N-(3-chloro-2-hydroxypropyl) trimethylammonium chloride (Quat188) were acquired from Tokyo Chemical Industry (Japan). Cellulose dialysis tubing (Membrane Filtration Products, USA), with a molecular weight cutoff of 12–14 kDa, was used to purify all modified chitosan samples. Milli-Q water was used for all experiments. All organic solvents (analytical grade) for reactions were purchased from Sigma-Aldrich (USA) and Merck (Germany).

3.3 Method

In this research, the methods are divided into four parts as shown in Fig 13. The first one is the study of the design and synthesis of derivatives used as a coating for the surface of AuNPs@collagen. The second part is the study of the synthesized gold nanoparticles using collagen as a reducing agent. The third part is the study of the coating on the surface of AuNPs@collagen using modified chitosan. The final part is

the study of the fabrication of 5-Fluorouracil drug loaded Bi-QCS-AuNPs@collagen and evaluation of its biological activity.
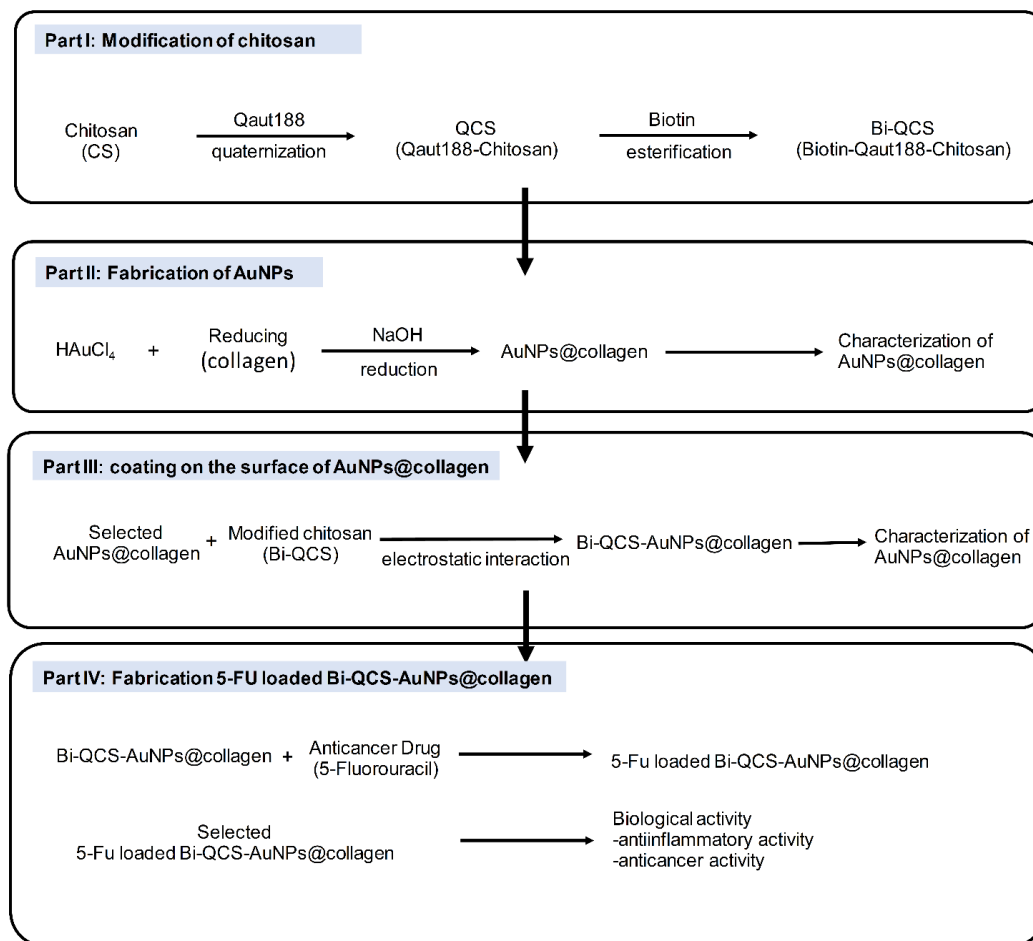
Figure 13 Experiment procedures are divided into four parts

Part I: Study of the design and synthesis of derivatives used as a coating for the surface of AuNPs@collagen

3.3.1 Modification of chitosan

Chitosan was modified to provide two structure features: (I) the positive charge from $-N^+(CH_3)_3$ of the quaternized chitosan (QCS) increase the electrostatic interaction with cell membrane, and (II) targeting molecule; biotin to specifically target receptor on the surface cancer cells, which is overexpression cancer cell as shown in Fig 14.
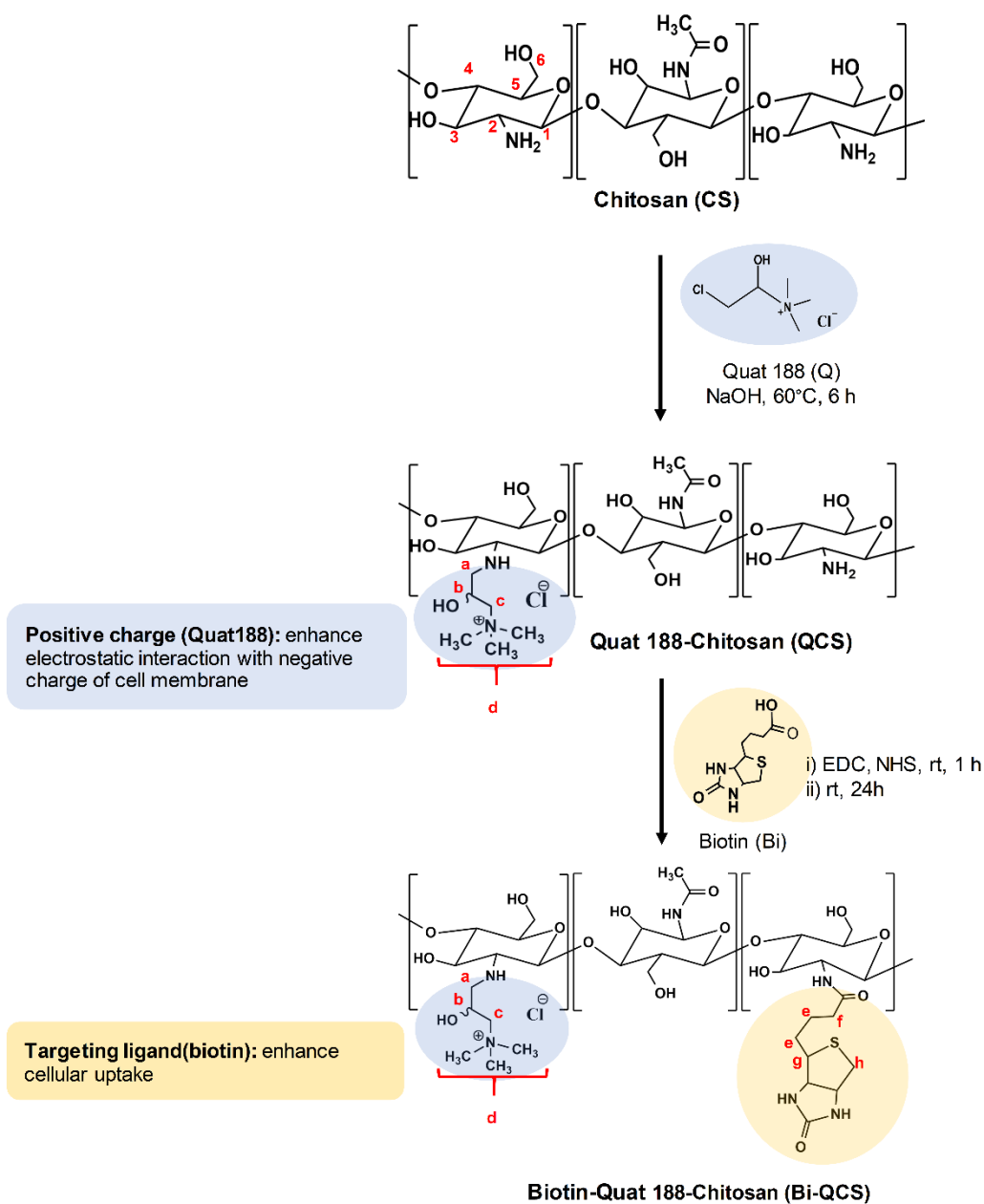
Figure 14 Schematic representation of the synthesis of Quat188-Chitosan (QCS) and Biotin-Quat188-Chitosan (Bi-QCS)

3.3.1.1 Synthesis of Quat188-chitosan (QCS)

Chitosan powder (1 g) was dissolved with 1 % (v/v) acetic acid solution (100 mL) at room temperature for overnight until completely dissolved. Then, the pH of the solution was adjusted to pH 9 using 15 % (w/v) aqueous sodium hydroxide. After that, 10 mL of 65 % (w/w) aqueous solution of N-(3-chloro-2-hydroxypropyl)-trimethylammonium chloride (Quat-188) were added to the reaction flask resulting in

the pH drop. The pH of the solution was then adjusted again to pH 8 using 15 % (w/v) sodium hydroxide. The solution was heat at 60 °C with a rigorous stirring for 6 h. Next, the mixture was precipitated in ethanol followed by dialysis against distilled water. Finally, the dialyzed solution was dried in the oven at 60 °C for 24 hour [70].

3.3.1.2 Synthesis of Biotin-Quat188-Chitosan (Bi-QCS)

Biotin (0.1 g, 0.41 mmol) was dissolved with dimethyl sulfoxide anhydrous (DMSO). Then, the solution was activated with EDC (0.25 g, 1.30 mmol) and NHS (0.15 g, 1.30 mmol) and stirred for 1 h at room temperature. After that, the activated biotin solution was added dropwise to 100 mL of 1 % (w/v) QCS in 1% (v/v) acetic acid solution and reacted for 24 h at room temperature. The mixture was precipitated in acetone followed by dialysis against deionized water for further 3 days to remove unreacted biotin. Next, the dialyzed solution was dried in the oven at 60 °C. After drying, biotinylated Quat188-chitosan (Bi-QCS) was obtained. The synthetic pathway and molecular structure of Bi-QCS are shown in Fig 14.

3.3.2 Calculation of degree of quaternization (%DQ) and biotin content

3.3.2.1 The degree of quaternization (%DQ) of Bi-QCS

Degree of quaternization (%DQ) of QCS was evaluated by ^{1}H NMR using Eq. (1) as previously reported [70].

$$\%DQ = \left[\frac{I(CH3)3}{I(H3-H6)} \times \frac{5}{9}\right] \times 100\% \tag{1}$$

Where $I_{(CH3)3}$ is the integral of the trimethyl amino group's protons of QCS (3.31 ppm), and $I_{(H3-H6)}$ is the integral of the H3-H6 protons of chitosan.

3.3.2.2 Determination of biotin content on the surface

Biotin content on the surface of Biotin-Quat188-chitosan (Bi-QCS) was determined by a biotin assay kit based on the company's protocol (Pierce Biotechnology, USA). The procedure was briefly described as follows: a total of 10 μL of each standard and/or sample was added to each well, and 90 μL of fluorescent

avidin with HABA (DyLight Reporter) that was added to the solution containing the biotinylated sample. The samples were incubated for 5 min. All samples were measured the fluorescence at excitation/emission 494/520 nm using a fluorescent microplate reader (Molecular Devices SpectraMax M2, USA). The amount of biotin in the sample is compared with the fluorescence to a biocytin standard curve [71].

Part II: Study of the synthesized gold nanoparticles using collagen as a reducing agent

3.3.3 Preparation of AuNPs@collagen

In this work, we studied the effect of various final concentrations of collagen (0.1, 0.5, 1 and 2.5 % (w/v) to synthesis AuNPs. Before the experiment, the stock solution for synthesis of AuNPs@collgen was prepared by 3mM of $HAuCl_4$, 10 % (w/v) of collagen, Bi-QCS in 1% acetic acid, and 5% sodium hydroxide (NaOH) in milli-Q water.

The Collagen functionalized AuNPs were synthesized by the reduction of chloroauric acid ($HAuCl_4$) as shown in Fig 15. Collagen was used as a reducing and stabilizing agent. In a typical reaction procedure, 50 µl of 10 % (w/v) collagen were mixed with 15 µl of 5 % (w/v) NaOH solution at 80°C for 20 min. Then, the pH of the mixed solution was adjusted to 9 with 5 % (w/v) NaOH. Next, 60 µl of 3 mM $HAuCl_4$ was added into the mixture. The solution was reconstituted to a final volume of 1 mL with milli-Q water. The reaction mixture was continuously stirred at 80 °C for 40 min. The color was changed from yellow to ruby red, which confirmed the formation of AuNPs@collagen. After that, the AuNPs@collagen were purified by centrifugation at 13,000 rpm for 10 min. The supernatant was discarded and the pallet was resuspended in water (1 ml). In this work, the concentration of collagen (0.1, 0.5, 1 and 2.5 % (w/v)) was varied to study the effect of collagen to control the morphology and particles size of AuNPs.
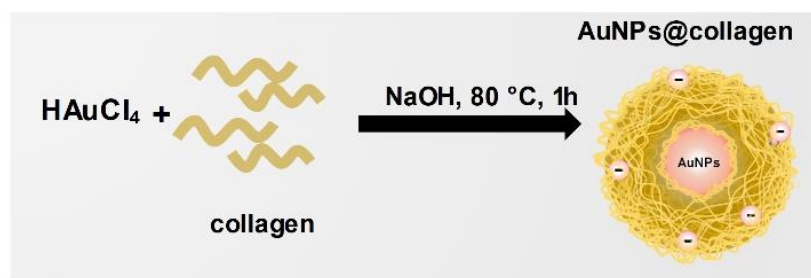
Figure 15 Preparation of AuNPs using collagen as a reducing agent

Part III: Study of the coating on the surface of AuNPs@collagen using modified chitosan

3.3.4 Fabrication of Bi-QCS-AuNPs@collagen

In this part, the optimum AuNPs@collagen to Bi-QCS ratio was evaluated. The coating of AuNPs@collagen with Bi-QCS: first, the AuNPS@collagen solution was adjusted the volume to 1 ml. Then, the Bi-QCS solution was added dropwise to the AuNPS@collagen solution to coat on the surface of AuNPS@collagen, while magnetically stirred at room temperature for 30 min. After that, the Bi-QCS-AuNPs@collagen were purified by centrifugation. The solution was stored at 4° C before loading of 5-fluorouracil (5-FU). The AuNPS@collagen were mixed with Bi-QCS at the different conditions to obtain Bi-QCS-AuNPs@collagen as shown in Table 1.

Table 1 Compositions of Bi-QCS-AuNPs@collagen formulations

Formulations	AuNPs@collagen (nM)	Bi-QCS (% w/v)	AuNPs@collagen/Bi-QCS ratio (% v/v)
T1	6.88	0.20	1:16
T2	6.88	0.30	1:16
T3	6.88	0.40	1:12
T4	6.88	0.50	1:8
T5	6.88	0.75	1:4

3.3.5 Characterization of AuNPs@collagen and Bi-QCS-AuNPs@collagen

The characterization of AuNPs@collagen and Bi-QCS-AuNPs@collagen was analyzed by HT-7800 transmission electron microscope (TEM), Agilent 8453 UV-vis spectrophotometer (UV-vis), Nicolet iS50 fourier transformed infrared spectroscopy (FTIR), Dynamic light scattering (DLS) method and zetasizer nano series. The concentration of Au was determined by Inductively coupled plasma atomic emission spectroscopy (ICP-AES) analysis.

The TEM (Hitachi HT-7800, Japan) was operated at 80 kV to analyze the morphology of the AuNPs@collagen and Bi-QCS-AuNPs@collagen. The samples were prepared by dropping 5ul of the dilute samples onto carbon-coated copper grids (Electron Microscope Science, USA). The samples were dried in desiccators for overnight. The absorption spectra of AuNPs@collagen and Bi-QCS-AuNPs@collagen was analyzed by UV-vis spectrophotometry (Agilent 8453). The FTIR spectra (Nicolet iS50) were operated in transmittance mode between 400 cm^{-1} and 4000 cm^{-1}. The particle size of the AuNPs@collagen and Bi-QCS-AuNPs@collagen was measured using a dynamic light scattering (DLS) method with a particle size analyzer at 25 °C. Moreover, the surface charge of prepared AuNPs@collagen and Bi-QCS-AuNPs@collagen was measured with a zeta potential value by electrophoretic light scattering using a zetasizer. The samples for analysis with DLS and zetasizer, were prepared by diluted with DI water (1:10 (v/v)). The concentration of Au was determined by Inductively coupled plasma atomic emission spectroscopy (ICP-AES, ICPE-9820 Shimadzu, Japan) analysis. The samples were digested in aqua regia, HCl: Nitric acid (3:1), and diluted in milli-Q water.

Part IV: Study of the fabrication of 5-Fluorouracil drug loaded Bi-QCS-AuNPs@collagen and evaluation of its biological activity

3.3.6 Preparation and characterization of 5-FU loaded Bi-QCS-AuNPs@collagen

For prepare 5-FU loaded Bi-QCS-AuNPs@collagen, the Bi-QCS-AuNPs@collagen solution was dispersed in 500 µl of 20 mg/ml 5-FU solution. Then, the mixture was

incubated at room temperature for 3 h followed by centrifuged at 7,000 rpm for 30 min. The presence of 5-FU loading was confirmed by UV-vis, FTIR and zeta potential analyses. The supernatant was analyzed by UV-visible absorption spectrum at 266 nm to determine the encapsulation efficiency of Bi-QCS-AuNPs@collagen. The encapsulation efficiency was calculated by the following equation:

$$\text{Encapsulation efficiency (\%)} = \frac{\text{Total 5-FU} - \text{Free 5-FU}}{\text{Total 5-FU}} \times 100 \qquad (2)$$

3.3.7 In vitro 5-FU release studies

The 5-FU release studies were carried out using the dialysis method. The 5-FU-loaded Bi-QCS-AuNPs@collagen solution (2 mL, 2.5 mg of 5-FU) was introduced into a dialysis bag (MWCO 3.5 kDa, MFPI, USA). The bags were placed in 50 mL of phosphate buffer pH 5.5 and 7.4 in the tightly closed tubes. The tubes were placed in an incubator shaker operating at a speed of 150 rpm and a temperature of 37 °C. The aliquots were withdrawn from the media at different time intervals and replaced by the same volume of fresh medium. Then, the concentrations of 5-FU in the samples were analyzed by UV-vis spectrophotometer at 266 nm. The cumulative percent of 5-FU released was plotted as a function of time.

3.4 Biological activities test

3.4.1 Anti-inflammatory activity of Bi-QCS-AuNPs@collagen

3.4.1.1 Cell culture

Murine macrophage cells line (RAW 264.7) was cultured in Dulbecco's Modified Eagle Medium (DMEM) (Gibco, USA) supplemented with 10 % (v/v) fetal bovine serum (FBS) (Gibco, USA), 1% (v/v) glutamax (Gibco, USA), 1 % (v/v) penicillin-steptomycin (Capricorn scientific , Germany), and incubated at 37°C in a humidified atmosphere containing 5% CO_2.

3.4.1.2 Assessment of the nitric oxide (NO) inhibition effect using Raw 264.7 cells

The inhibitory effect on NO production in RAW 264.7 cells was evaluated using a Singh method [72]. Briefly, 2×10^5 cells/well were seeded in 96-well plates. After 24 h, the medium was replaced with fresh medium containing 1 μg/ mL of lipopolysaccharides (LPS) (Sigma-Aldrich, USA). The samples at various concentrations were added into the cells, and incubated for 24 h. NO production was determined by measuring the accumulation of nitrite in the culture supernatant using the Griess reagent (Sigma-Aldrich, USA) with a microplate reader at the wavelength of 540 nm. The percentage of inhibition (%) was calculated by the Eq. (3) [73]:

$$\text{Inhibition (\%)} = \frac{C - T}{C} \times 100 \qquad (3)$$

Where *C* is absorbance of the control and *T* for the test samples.

3.4.2 Anticancer activity of 5-FU loaded Bi-QCS-AuNPs

3.4.2.1 Cell culture

Lung cancer cells (A549) was cultured in RPMI-1640 medium (Gibco, USA) supplemented with 10 % (v/v) fetal bovine serum (FBS), 1 % (v/v) glutamax, and 1 % (v/v) penicillin-steptomycin. The cervical cancer (HeLa) and fibroblast (normal cell) were grown 95% relative humidity in DMEM supplemented with 10 % (v/v) fetal bovine serum (FBS), 1 % (v/v) glutamax, and 1 % (v/v) penicillin-steptomycin. The cultured cells were incubated in 5% CO_2 at 37°C.

3.4.2.2 Cytotoxicity study

In order to determine the cytotoxicity of free 5-FU and 5-Fu loaded Bi-QCS-AuNPs@collagen, MTT assay was applied. The evaluation of cytotoxicity was based on the reduction of 3-(4,5-dimethylthiazol-2-yl)-2,5-diphenyltetrazolium bromide dye (MTT) (EMD Millipore, USA) by viable cells to generate purple formazan products, which were measured spectrophotometrically at wavelength 570 nm. Fibroblast and cancer

cells were seeded into 96-well plates at 10,000 cells/well separately and incubated at 37 °C. After 24 h, the cells were treated with various concentrations of compounds for 48 h. Then, 100 µL of MTT solution (0.5 mg/mL) was added, and incubated for 3 h. Finally, the media were removed followed by solubilized the formazan crystals in 100 µL of DMSO and analyzed by UV-Vis spectrophotometry at the wavelength of 570 nm [74]. The cell viability for each compound was calculated by the following equation [75]: The IC_{50} values, the concentration of an inhibitor that reduces the response by half, were determined.

$$\text{The cell viability (\%)} = \frac{A}{B} \times 100 \qquad (4)$$

Where A and B were the absorbances of the experimental and control cells, respectively.

3.5 Statistical analysis

All experiments were conducted in triplicate and the results are presented as mean ± standard. Depending on the number of the sample for comparison, the statistical significance was determined using two-tailed Student's t test or one-way analysis of variance (ANOVA) with Tukey's post-hoc test. The p-value of lower than 0.05 were considered as significant difference. The graphs were plotted using the GraphPad Prism 5 software.

CHAPTER IV
RESULTS AND DISCUSSION

Gold nanoparticles (AuNPs) are one of the most popular drug carriers for the drug delivery system. Due to the unique properties consist of low cytotoxicity, tunable size, and biocompatibility [3]. Moreover, the highly tunable and multivalent surface structures of AuNPs affect a variety of functionalization. The ability to tailor the surface has made AuNPs effective in both active and passive targeting [4]. Nowadays, there have a variety of AuNPs synthesis methods, the most common method is a chemical method. Among the chemical synthesis category, the Turchevich-Frens and Brust-Schriffin methods are the most widely known and use [5, 6]. However, this technique has several disadvantages such as reproducibility, toxic chemical, and difficult steps. Due to these drawbacks, the green synthesis methods (biopolymer) are attractive because of the less toxicity, biocompatibility, controller of the drug release, and uncomplicated synthesis method.

Even though the green methods produce less toxic nanoparticles, there still needs more optimization of drug encapsulation efficiency on AuNPs surface and the stability [9]. In the same way, the surface of gold nanoparticles as the type of monolayer or multilayer has been applied to improve stability and drug encapsulation efficiency [10]. We reported herein polyelectrolyte coated AuNPs (Bi-QCS-AuNPS@collagen) with greater 5-FU loading compared to those traditional gold nanoparticles. The Bi-QCS-AuNPS@collagen was designed as follow: (i) collagen, a negative charge polymer, was used as a reducing agent and a stabilizing agent of the AuNPs, (ii) quaternized chitosan (QCS), a positive charge polymer, was coated in the outer layer of AuNP@collagen, (iii) biotin, a targeting molecule was conjugated with QCS to increase cellular uptake and control drug release of the particles. Bi-QCS-AuNPS@collagen and 5-FU-loaded Bi-QCS-AuNPS@collagen were characterized and evaluated for their safety profile, anti-inflammation, cancer suppression in vitro. The layer-by-layer coating of the nanoparticles was designed to enhance 5-FU loading due to strong electrostatic interaction and H-bonding. It is also highlighting that

Bi-QCS-AuNPS@collagen is a pH-sensitive nanoparticle, which can prevent premature release in a normal physiological pH but rapidly release the drug in an acidic condition in endosome and tumor microenvironment. In this chapter, the result and discussion are presented.

Part I: Study of the design and synthesis of derivatives used as a coating for the surface of AuNps@collagen

Chitosan was modified to provide two structure feature: (I) the positive charge from $-N^+(CH_3)_3$ of the quaternized chitosan increase the electrostatic interaction with cell membrane; QCS (II) targeting molecule, biotin to specifically target receptor on the surface cancer cells, which is overexpress on cancer cell; Bi-QCS, as shown in Fig 16.

Biotin-Quat 188-Chitosan (Bi-QCS)
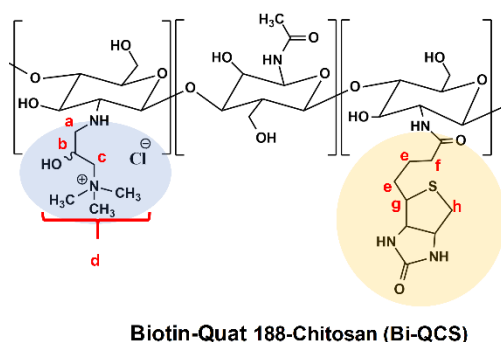
Figure 16 Molecular structure of modified chitosan (Bi-QCS)

4.1 Synthesis and characterization of modified chitosan (Bi-QCS)

4.1.1 FTIR

The synthesis of Bi-QCS was carried out by the quaternization using Q188 reacted with both the primary amine and hydroxyl groups of chitosan. Afterwards, biotin was attached though coupling of the carboxylic groups to the available primary amine groups of QCS using an EDC and NHS reaction. Then, the Bi-QCS was analyzed by FTIR and ^{1}H NMR to confirm the presence of biotin Quat188 on the chitosan. The FTIR spectrum of chitosan, QCS, and Bi-QCS are shown in Fig 17. The FTIR of chitosan showed a broad absorption at 3,434 cm^{-1}, attributed to O-H and N-H stretching. The

absorptions at 1,653 cm^{-1} and 1,595 cm^{-1} are assigned to C=O stretching of amide I and N-H bonding of amide II, respectively. Moreover, the broad absorption at 1,020-1,160 cm^{-1} region is related to the polysaccharide skeleton of C-O-C stretching and the vibration of C-O stretching. The spectrum of QCS presented a new peak at 1,468 cm^{-1}, which is attributed to C-H asymmetric stretching of methyl groups. After the conjugation of biotin with QCS, the FTIR spectrum of biotin appeared at 1,685 cm^{-1} (the C=O stretching vibration of carboxyl group), while the peak at 1,641 cm^{-1} assigned to the C=O bond stretching vibration of -CO-NH group. However, the C=O stretching vibration of the amide bond shifted from 1,641 to 1,538 cm^{-1} of the Bi-QCS that confirmed the existence of chemical interactions between biotin and QCS. These results indicated that the biotin was successfully conjugate onto the QCS to obtain Bi-QCS.
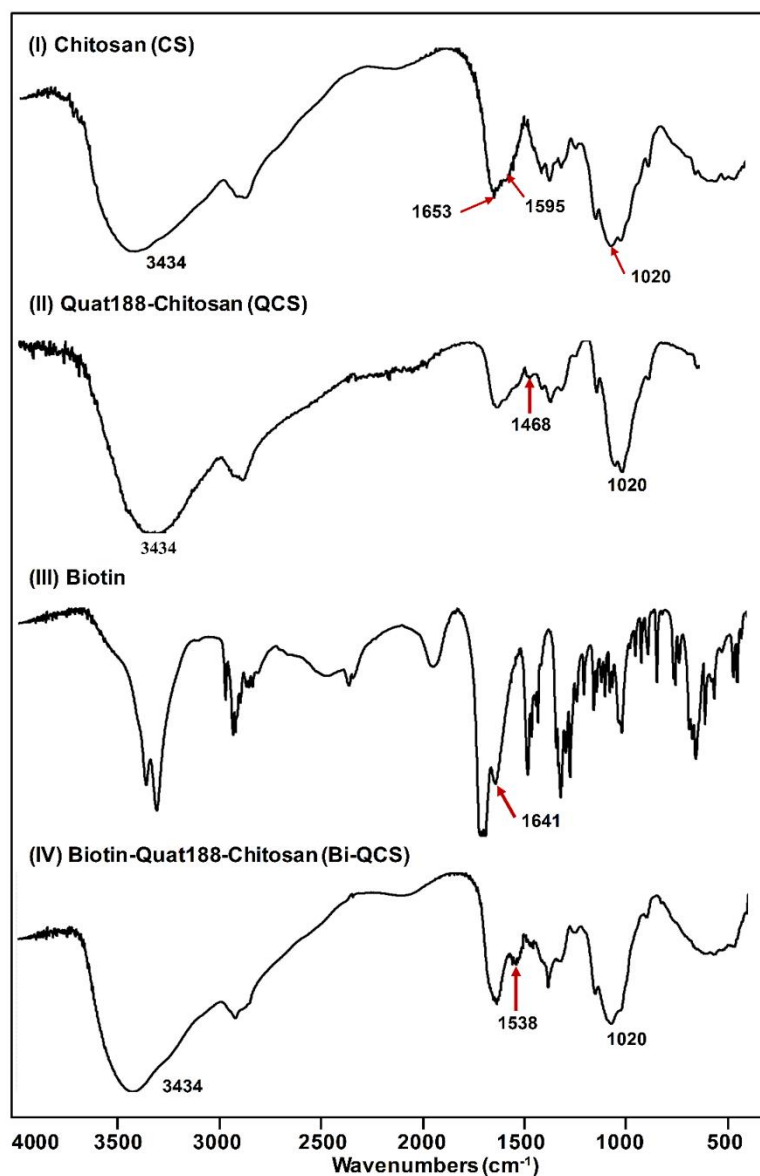
Figure 17 FTIR spectra of (I) Chitosan (CS), (II) Quat188-Chitosan (QCS), (III) Biotin, and (VI) Biotin-Quat188-Chitosan (Bi-QCS)

4.1.2 ^{1}H NMR

The ^{1}H NMR of chitosan showed the signals of the H3-H6 protons of approximately 3.80-3.40 ppm (corresponding to the pyranose ring), the H2 proton of 2.95 ppm (corresponding to the acetyl), and the proton of N-acetylglucosamine unit at 1.84 ppm. After quaternization, the ^{1}H NMR spectrum of QCS appeared a new peak consist of at 3.08 ppm for the N,N,N-trimethyl amino group's ((CH_3)$_3N^+$; d), 3.31 ppm

for the methylene protons ($CH_2N^+(CH_3)_3$; c), 2.52 ppm for the methylene protons (CH_2; a) and 4.46 ppm for methine protons (CHOH; b) [76]. The DQ of QCS was determined by ^1H NMR spectroscopy with calculations according to Eq. (1), which was approximately 24.44%. The ^1H NMR spectrum of Bi-QCS identified the new signals including methylene protons at 1.25-1.6 ppm (6H; e), 2.14 ppm (2H; f), methine protons at 4.19 ppm (1H; g), and 4.22 ppm (1H; h). Moreover, the characteristic signals of biotin were relatively weak because of its low content in the biotinylated polymer (as shown in Fig 18) [77]. The content of biotin of Bi-QCS is 482.63 ± 0.45 pmol/µl (11.81%) determined by the biotin assay kit.
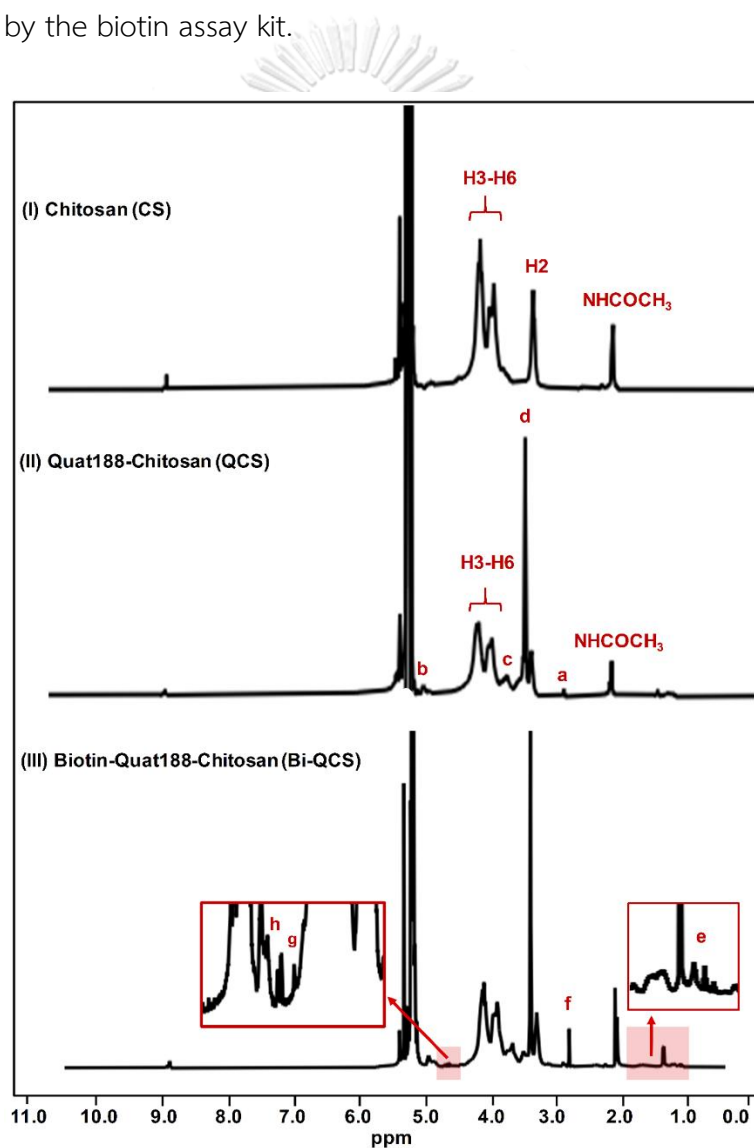
Figure 18 ^1H NMR spectra of (I) Chitosan (CS), (II) Quat188-Chitosan (QCS), and (III) Biotin-Quat188-Chitosan (Bi-QCS)

Part II: Study of the synthesized gold nanoparticles using collagen as a reducing agent

4.2 Synthesis and characterization of AuNPs@collagen

The AuNPs@collagen (as illustrated in Fig 19) was synthesized by the reduction of $HAuCl_4$ with type I collagen, which acts as a reducing and stabilizing agent. The generation mechanism of the negative charge AuNPs was proposed in which type I collagen has created reducing species under alkaline treatment (pH 8.5-9) to reduce Au^{3+} to Au^0. NaOH acts as a catalyst in the reaction to deprotonate the carboxyl group and to protonate the amine groups of type I collagen, which generates higher reducing power to produce AuNPs. The formation of the AuNPs@collagen was confirmed by the change of the color of solution from yellow to ruby red. Moreover, the type I collagen concentrations affect the control of particle size distribution and morphology of the AuNPs@collagen.
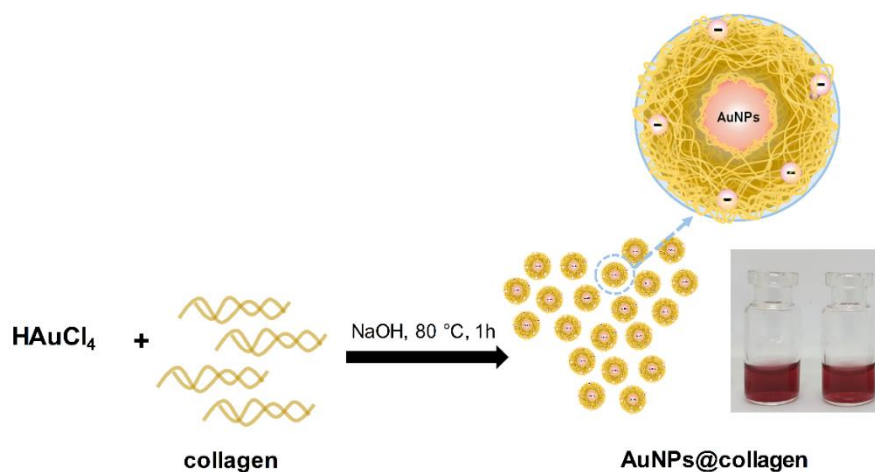
Figure 19 Preparation and proposed structure of AuNPs@collagen

4.2.1 Effect of type I collagen concentration

The effect of collagen concentrations on the synthesis of AuNPs@collagen was studied in the various collagen concentrations (0.1, 0.5, 1, and 2.5 % (w/v)) resulting in the color changes of the solution from a yellow solution ($AuCl_4^-$) to red, ruby red, purple, and blue (Au^0), respectively. This is attributed to the oscillation of free

electrons induced by an interacting electromagnetic field in AuNPs, which is known as the localized surface plasmon resonance (LSPR) [78]. The LSPR at 520 and 650 nm corresponded to smaller-sized and larger-sized AuNPs, respectively [79].

At concentrations of 0.1, 0.5, 1, and 2.5 % (w/v) of collagen showed the maximum absorptions at 526, 525, 530, and 559 nm, respectively (Fig 20a). 0.5 % (w/v) of collagen exhibited the highest A650/A520 ratio among all concentrations, which presented the highest amount of gold nanoparticles as shown in (Fig 20b) with a narrow size distribution and no particle aggregation. It is explained that the amino acids in the collagen can reduce $AuCl_4^-$ to Au^0. Especially, aromatic amino acids are strong reducing agents for AuNPs, in which the carboxyl groups scavenge radicals to $\bullet CH_2COOH$ (or $\bullet CH_2COO^-$; a reducing radical). The amine and carboxyl groups of amino acids in collagen not only play an important role in the reducing of $AuCl_4^-$ but also stabilizing the nanoparticle [80].

Whereas, 0.1 % (w/v) of collagen concentration showed a weak LSPR intensity of AuNPs formations due to the low concentration of collagen and insufficient reducing power, while the concentrations higher than 0.5 % (w/v) of collagen showed precipitation and the broad peak at the 560 nm due to the entanglement of the particles. Therefore, the optimal concentration of the collagen is 0.5 % (w/v). The DLS of the optimal concentration condition confirms the average size of 39.73 ±0.02 nm with the zeta potential of -32.1 mV. The TEM images of AuNPs@collagen indicate the average diameter of 27 nm. Moreover, the concentration of AuNPs@collagen is 6.88 nM measured by an ICP-AES technique.
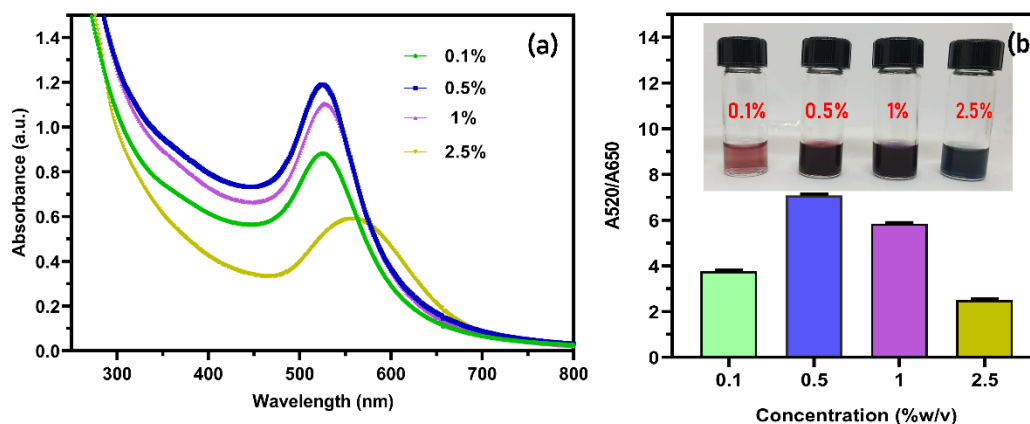
Figure 20 (a) UV-vis spectra and (b) a plot of the intensity ratio between λ_{max} at 620 and 520 nm of AuNPs@collagen after synthesis at different concentration.

Part III: Study of the coating on the surface of AuNPs@collagen using modified chitosan

4.3 The study of the optimal Bi-QCS ratios for layer-by-layer AuNPs@collagen coating

After successful synthesis of AuNPs@collagen, we coated Bi-QCS on the surface of AuNPs@collagen and optimized the conditions to prepare for drug loading. Considering the specific case of coating on the surface of AuNPs containing collagen and chitosan, it generally found an electrostatic interaction between the negatively charged collagen and the positively charged chitosan to form a complex. Moreover, the concentrations of the Bi-QCS directly affects the stability of the AuNPs@collagen.

In order to investigate the control of the stability and efficiency of Bi-QCS in AuNPs@collagen surface covering, the effect of the appropriate concentrations and ratios on particle coating was studied as shown in Table 2. The suitable formulations were considered based on size and surface charge. Low concentrations of Bi-QCS (T1 and T2) generate less positive zeta potential (< 20 mV) resulted in the lower stability of AuNPs@collagen because of insufficient covering on the surface of AuNPs@collagen. This induced the aggregation of the particles.

In contrast, the stability of AuNPs@collagen significantly improved with the increasing Bi-QCS concentration due to an increasing coverage on surface of AuNPs@collagen. However, 0.75 % (w/v) (T5) Bi-QCS yields a large size of particles approximately 273 nm and with > 40 mV of the zeta potential, which may result in lower cellular uptake and cytotoxicity. Therefore, this formula (T5) was unsuitable for drug delivery.

Meanwhile, T3 and T4 had a size range of approximately 70-101 nm. It has been reported that the suitable size of nanoparticles for the cancer treatment is approximately 50-100 nm because it can fully take advantages of the enhanced permeability and retention (EPR) effect in the tumor sites [81] and also avoid capture by macrophages in the reticuloendothelial system (RES) [82]. While The zeta value of T4 (34.8 mV) is greater than T3 (38.6 mV) (as described in Table 2) indicating a strong interparticle electrostatic repulsion between the nanoparticles resulting in a better prevention against nanoparticle aggregation. While the difference of the particle sizes of T3 and T4 does not significantly impacted the stability of the nanoparticles. Therefore, T3 was selected for further experiments.

Table 2 Effect of the concentrations of Bi-QCS coated on AuNPs@collagen

Formulations	PDI	Particle size (nm)	Zeta potential (mV)
T1	0.38	277.77 ± 25.20	16.8
T2	0.33	243.10 ± 79.17	18.9
T3	0.27	101.24 ± 0.91	38.6
T4	0.39	74.01 ± 28.80	34.8
T5	0.35	273.13 ± 12.97	44.4

Data are represented as mean ± SD deviation (n=3).

The Bi-QCS coating layer of AuNPs@collagen was confirmed by a slight shift of LSPR from 525 nm to 527 nm. Moreover, there is no broad peak at 650 nm, indicating no aggregation of AuNPs@collagen as shown in Fig 21.
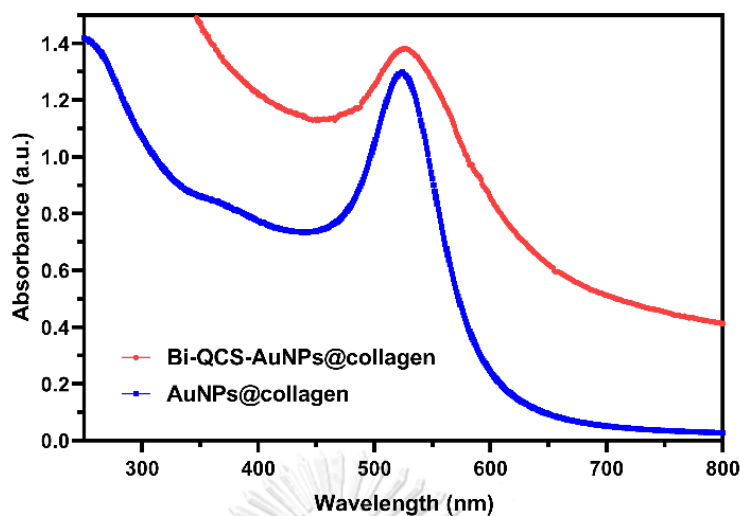
Figure 21 The spectra of AuNPs@collagen and Bi-QCS-AuNPs@collagen

The characterization of Bi-QCS-AuNPs@collagen was analyzed by FTIR as shown in Fig 22. The FTIR spectra of AuNPs@collagen observed at 1,018 and 1,115 cm^{-1} generally described to C-O vibrations from glycosidic side chain from collagen. The FTIR spectra of Bi-QCS appeared absorption peak at 1,653 cm^{-1} (C=O stretching of amide I) and 1,390 cm^{-1} (C-H and O-H bending vibration of amide II). The adsorption of Bi-QCS onto AuNPs@collagen surface showed a shift in characteristic peak of Bi-QCs polymer to 1,642 cm^{-1} and 1,418 cm^{-1}, respectively. It indicated the successfully Bi-QCS coated onto AuNPs@collagen via the electrostatic interaction of the amine group of Bi-QCS and the carboxyl group in collagen on the surface of AuNPs.
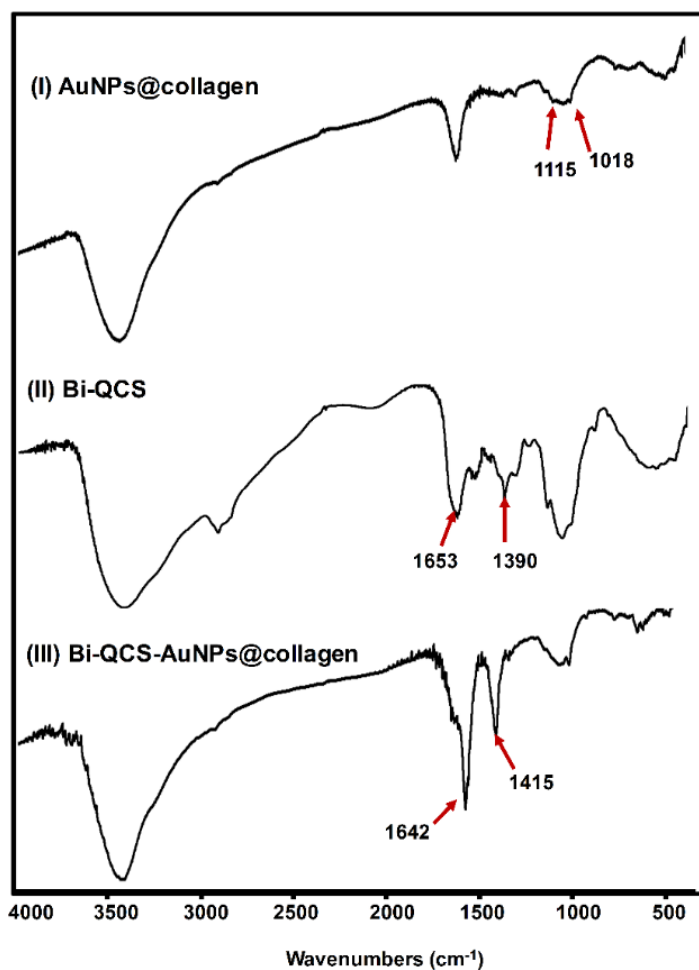
Figure 22 The FTIR spectrum of (I) AuNPs@collagen, (II) Bi-QCS, and (III) Bi-QCS-AuNPs@collagen

4.4 Characterization of Bi-QCS AuNPs@collagen

The average particle size of AuNPs@collagen determined by a dynamic light scattering technique was 39.75 ± 0.02 nm (PDI: 0.20 ± 0.05), and increased to 101.24 ± 0.9 nm (PDI: 0.27 ± 0.09) after coated with Bi-QCS (T3 formulation) (as shown in Fig 23a). The zeta-potential of AuNPs@collagen was -32.1 ± 5.4 and changed to 38.6 ± 0.12 mV after coating with Bi-QCS (as shown in Fig 23b).

The TEM images of AuNPs@collagen indicate the average diameter of 27-30 nm approximately (as shown in Fig 23c). After coating Bi-QCS on the surface of AuNPs@collagen was observed at approximately 47-52 nm (as shown in Fig 23d). The

average thickness of the Bi-QCS shell on the AuNPs@collagen core measured from TEM images was 7 nm. The diameters of Bi-QCS-AuNPs@collagen determined by DLS (Fig 23a) is larger than the average diameter measured TEM by because the DLS technique provides the hydrodynamic radius of the nanoparticles in aqueous media, whereas TEM is only sensitive to electron-rich particles in a dry state (Kong et al., 2014).
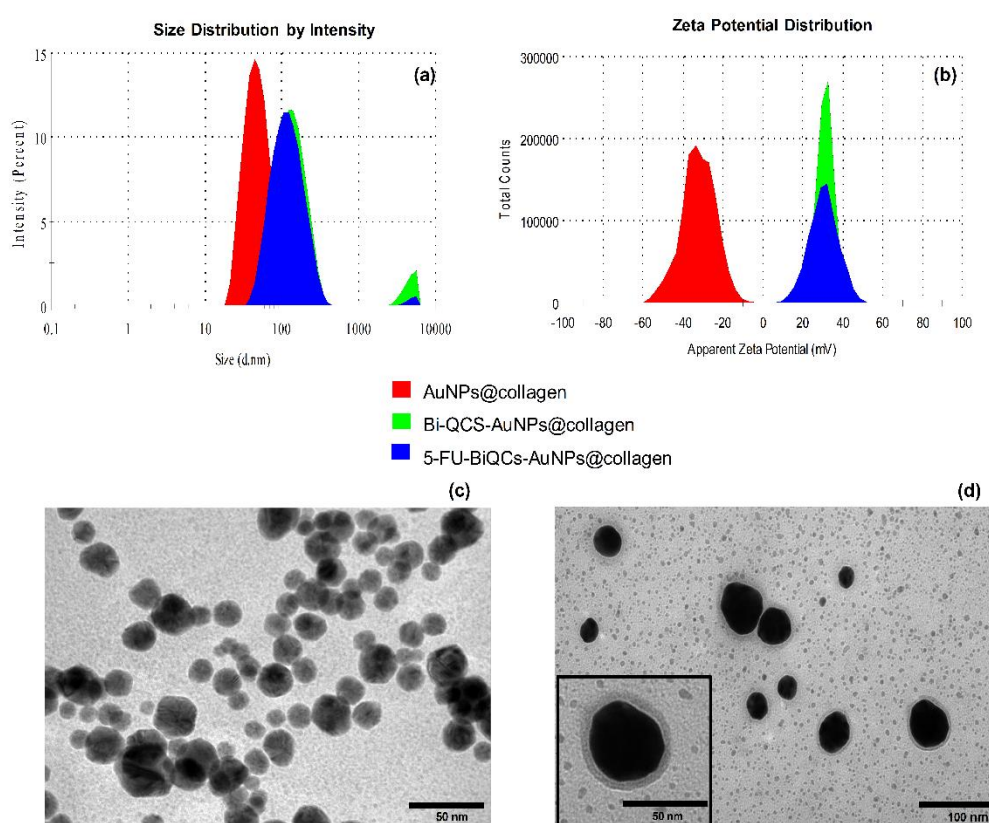
Figure 23 (a) Size distribution from DLS analysis, (b) zeta potential and (c) TEM image of AuNPs@collagen and (d) after successfully coating with Bi-QCS. Data are represented as mean ± SD deviation (n=3).

Part IV: Study of the fabrication of 5-Fluorouracil drug loaded Bi-QCS-AuNPs@collagen and evaluation of its biological activity

4.5 Synthesis and characterization of 5-FU loaded Bi-QCS-AuNPs@collagen

In the previous study, we were successfully prepared Bi-QCS coated surface of AuNPs@collagen for the drug loading step. 5-FU-BiQCS-AuNPs@collagen was prepared

by the loading of 5-Fluorouracil into BiQCS-AuNPs@collagen. The pH of the solution was optimized due to the limited solubility of chitosan at higher pH condition. When the pH is above its pKa (6.3), it tends to lose its charge and precipitates due to deprotonation of the amino groups. In contrast, 5-FU is negatively charged, and the pKa is in a range of 7.0-8.0. Therefore, the condition for loading 5-FU into Bi-QCS-AuNPs@collagen was selected at pH 6.5-7.0, in which Bi-QCS was still able to dissolve in water and precipitation was not found. QCS is one of the water-soluble chitosan derivatives. Moreover, QCS also contains many quaternary ammonium groups (permanently cationic) [70]. This property make Bi-QCS maintain its charge in this condition. Then, the 5-FU loaded Bi-QCS-AuNPs@collagen was analyzed by DLS, Zeta potential, and FTIR to confirm the presence of 5-FU. Finally, it was determined the encapsulation efficiency of 5-FU by using UV-Vis spectroscopy.

The hydrodynamic diameter of the particle was increased from 101.24 ± 0.9 nm (PDI: 0.27) to 109 ± 0.83 nm (PDI: 0.31) with a narrow PDI value (< 0.3), indicating the uniformity of particle sizes. However, the zeta potential decreased from 38.6 ± 0.12 mV to 25 ± 0.05 mV, which confirmed the loading 5-FU in Bi-QCS-AuNPs@collagen. Moreover, the interaction of 5-FU loading to Bi-QCS-AuNPs@collagen was confirmed by FTIR. The characteristic peak of 5-FU (as shown in Fig 24) at 1,427 cm^{-1}, which corresponds to C-H symmetric deformation on C=C [83]. In addition, the peak at 641 cm^{-1} was attributed to the C-H out of plane vibration of CF=OH and the N-H bonding appeared at 1,671 cm^{-1}. The spectrum of 5-FU-BiQCS-AuNPs@collagen shifted from 1,671 cm^{-1} to 1,633 cm^{-1}. This peak confirmed the bonding of 5-FU on the Au@collagen [83]. The ammonium group of the 5-FU associated with carboxyl group on the surface Bi-QCS-AuNPs@collagen through electrostatic interactions. Furthermore, the molecular arrangement of Bi-QCS and 5-FU was expected to be bonded with H-O-H through hydrogen bonding interaction [83]. These results confirmed the attractive forces including electrostatic and hydrogen bonding intermolecular interaction.
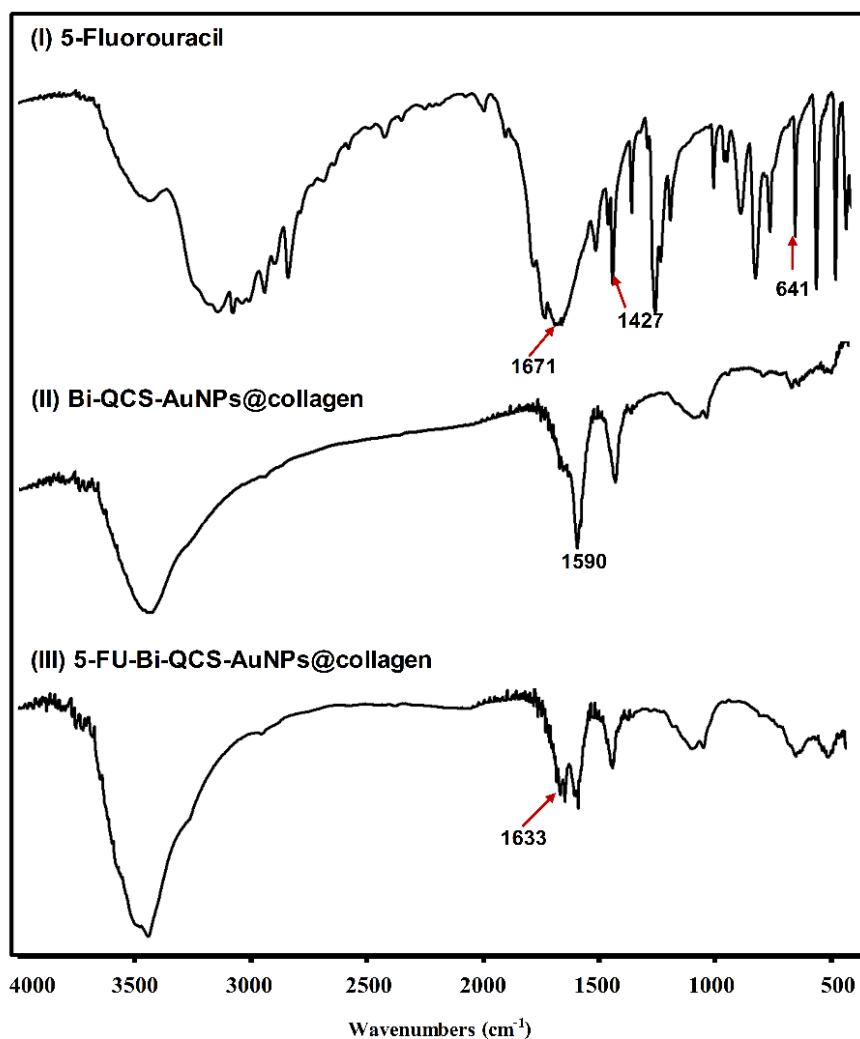
Figure 24 The FTIR spectra of 5-FU loaded Bi-QCS-AuNPs@collagen

The 5-FU encapsulation efficiency was compared between the drug encapsulation of 5-FU on the particles without polymer coating (AuNPs@collagen) and polymer coating (Bi-QCS-AuNPs@collagen). The encapsulation efficiency of Bi-QCS-AuNPs@collagen was 87.46 ± 0.21 %, while it was only 64.67 ± 0.46 % in the AuNP@collagen (as shown in Fig 25). Thus, Bi-QCS coating on AuNPs@collagen proved to increase the drug encapsulation efficiency on the surface AuNPs.
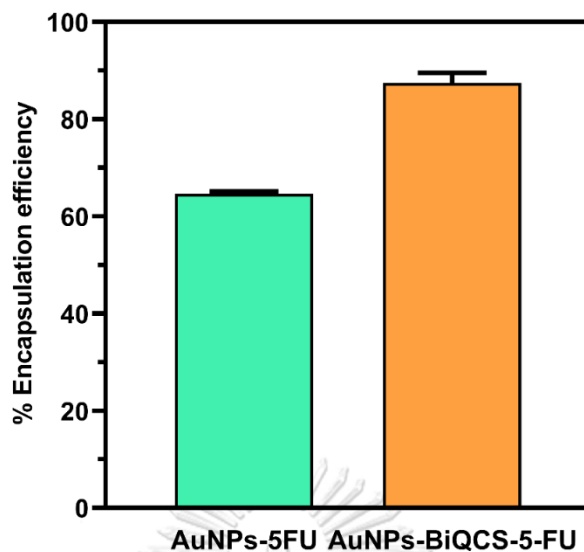
Figure 25 The encapsulation efficiency (%) of 5-FU compares with AuNPs@collagen and Bi-QCS-AuNPs@collagen. Data are represented as mean ± SD deviation (n=3).

4.6 *In vitro* drug release studies

5-FU released from Bi-QCS-AuNPs@collagen was studied in the PBS solution at pH 7.4 which represents the normal physiological pH, and at pH 5.4 which imitates the intracellular vesicles such as endosomes and lysosomes and microenvironment of cancer cells. The quantity of 5-FU released from the Bi-QCS-AuNPs@collagen was evaluated by using the UV-vis spectra. The free 5-FU solution used as a control was released rapidly and completed within 4 h at pH 5.4 and pH 7.4. In contrast, the release of 5- FU was slower in the Bi-QCS-AuNPs@collagen than the free 5-FU indicating that Bi-QCS-AuNPs@collagen could controlled the release rate of 5-FU. 5-FU-Bi-QCS-AuNPs@collagen also showed a significantly enhanced 5-FU release rate at pH 5.4 comparing to pH 7.4. The cumulative release amount of 5-FU from Bi-QCS-AuNPs@collagen at pH 7.4 was 39.6 % within 24 h and 42 % at 48 h, whereas the release rate at pH 5.4 was 60 % at 24 h and 71 % at 48 h. After 24 h, the release rates were slow down in both pH. (as shown in Fig 26). The chitosan is known to exhibit the pH-dependent swelling and controlled drug release properties [84]. At pH 7.4, the chitosan is orderly aggregated due to the deprotonation of its amino groups to prevent the release of 5-FU from the nanoparticles, while At pH 5.4, the protonated behavior

of the amino groups enables chitosan to dissolve and swell resulting in the release of 5-FU from Bi-QCS-AuNPs@collagen. The pH sensitive particles are known to be very useful for controlled drug release in cancer treatments due to less off-target and low adverse drug reactions.
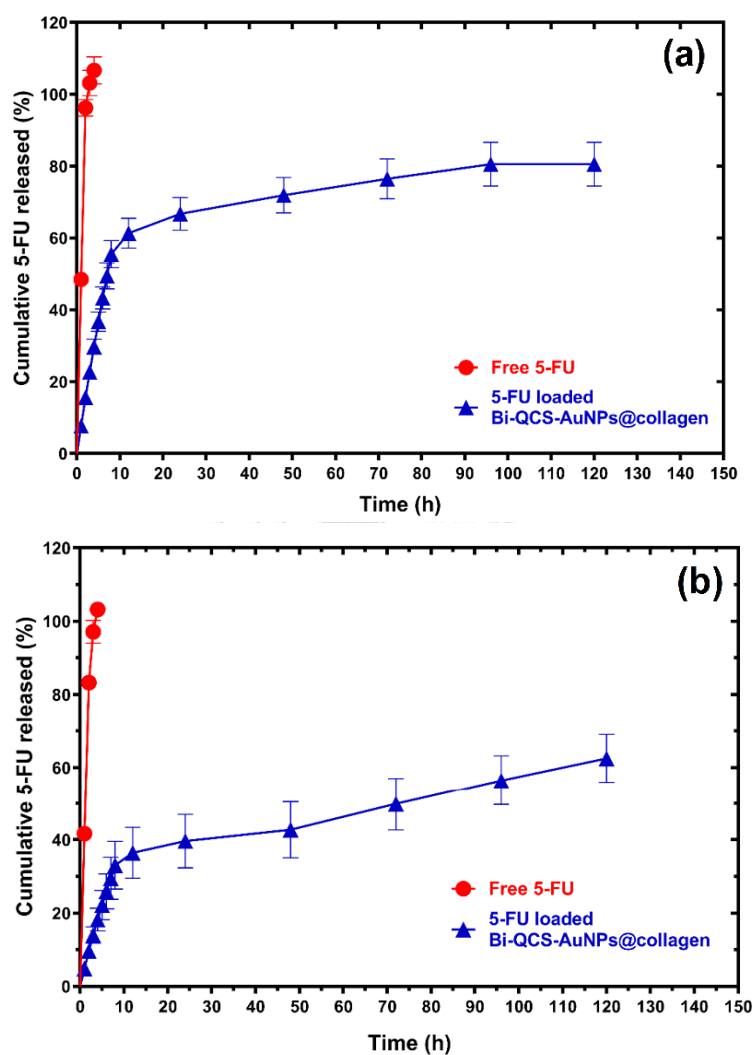
Figure 26 In vitro release profile of 5-FU- Bi-QCS-AuNPs@collagen and free 5-FU in PBS solution at pH (a) 5.4 and (b) 7.4. Data are represented as mean ± SD deviation (n=3).

4.7 Biological activities test

4.7.1 Anti-inflammatory activity

The cellular inflammation is involved in vascular tissue in responses to harmful stimuli such as damaged cells, irritants, and pathogens. In the pathogenesis of

inflammation, the overexpression of different cytokines such as COX-2, inducible nitric oxide synthase (iNOS), prostaglandin E2 (PGE2), interferon-grammar (IFN-γ), interleukin 1-beta (IL-1β) and tumor necrosis factor-alpha (TNF-α), are produced by activated macrophages [85]. Lipopolysaccharide (LPS), a well-known component of the cell wall of gram-negative bacteria, stimulates the inflammation inside the cell [86]. In this work, we studied the anti-inflammatory activity of Bi-QCS-AuNPs@collagen at different concentrations. The NO production in the supernatant was measured using Griess reagent (as shown in Fig 27). Dexamethasone, an anti-inflammatory drug, was used as a positive control (the inhibition was 80.60%). The NO inhibition by Bi-QCS-AuNPs@collagen at different concentration (0.005, 0.01, 0.02, 0.04, 0.09, 0.18, and 0.35 nM) indicating the inhibitory efficacy was 8.55, 12.82, 39.97, 43.38, 60.28, 68.63, and 73.87 %, respectively which significantly exhibiting strong anti-inflammatory activity ($p < 0.05$). The anti-inflammatory activity was increasing in a concentration-dependent manner.

The previous studies have described the anti-inflammatory pathway of the collagen. Collagen contains –OH and –NH_2 groups, which have the ability to bind to nitric oxide radical and lipoxygenase to inhibit produce these substances lipoxygenase. Nitric oxide and lipoxygenase play an important role in the synthesis of leukotrienes, which are mediators of several allergic and inflammatory conditions [87, 88]. Moreover, the high molecular weight chitosan has reported inhibiting the production of pro-inflammatory cytokines (TNF-α and IL-1) in human astrocytoma cells [89]. Apart from chitosan and collagen, gold nanoparticles (GNPs) also have presented antiinflammatory activity. The GNPs dose at 1,500 mg/kg exhibited a 49% reduction in leukocyte migration, which attested to the activation of a cellular anti-inflammatory response. These findings were also confirmed by the reduction of proinflammatory cytokines IL-1 beta and TNF-alpha [90].
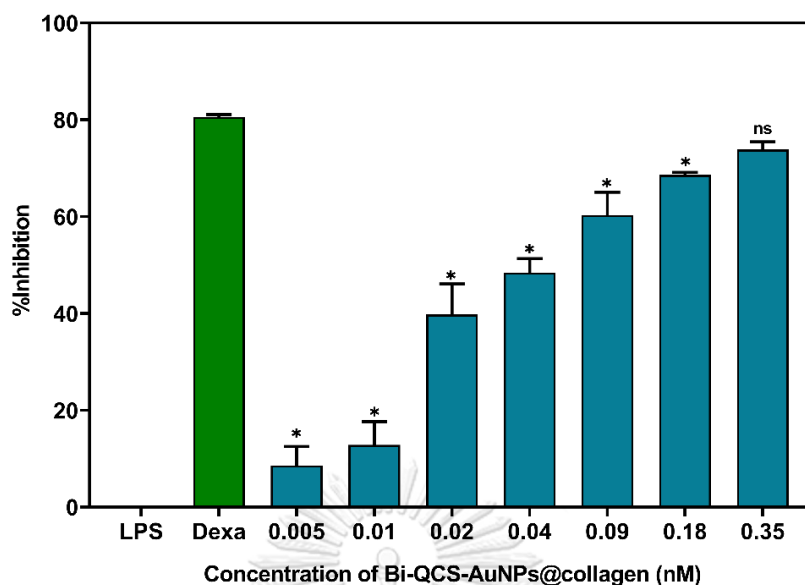
Figure 27 Effect of dexamethasone (Dexa) and the concentrations of Bi-QCS-AuNPs@collagen on NO production in RAW 264.7 cells induced by LPS. Data are represented as mean ± SD deviation (n=3). The asterisk (*) indicates a significant difference (p<0.05) compare with Dexa.

4.7.2 *In vitro* cytotoxicity assay of Bi-QCS-AuNPs@collagen and anti-cancer property of 5-FU-Bi-QCS-AuNPs@collagen

In order to examine the safety of Bi-QCS-AuNPs@collagen, the MTT assay was performed in fibroblast cells. The cytotoxicity of Bi-QCS-AuNPs@collagen in fibroblasts has proportionally increased based on the concentrations of the particle. The cell is likely to tolerate well at the concentrations ranging from 0.005 nM to 0.175 nM. The fibroblast cell viability is approximately 73.14% at 0.175 nM as shown in Fig 28, This assay proved that Bi-QCS-AuNPs@collagen in this range is safe to use. Therefore, the Bi-QCS-AuNPs@collagen at a 0.175 nM was used for loading 5-FU.
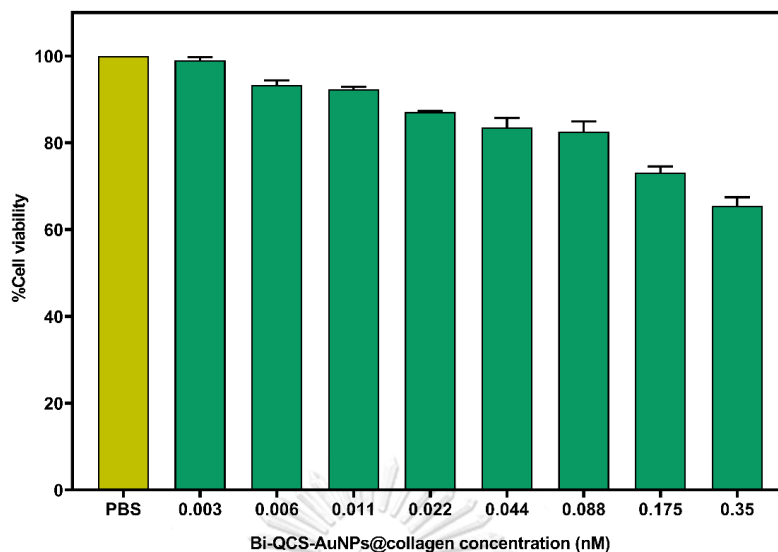
Figure 28 Effect of the concentrations of Bi-QCS-AuNPs@collagen on the fibroblast cell viability.

Next, the anticancer activities of 5-FU loaded Bi-QCS-AuNPs@collagen and free 5-FU were examined against cervical cancer (HeLa) and lung cancer (A549) using the MTT assay. The percent cell viability of HeLa and A549 after treatment with 5-FU-Bi-QCS-AuNPs@collagen was shown in Fig 29a and 29b. The IC_{50} of 5-FU-Bi-QCS-AuNPs@collagen against HeLa cells was 262.68 ± 5.79 µM compared to free 5-FU (902.86 ± 10.77 µM). Likewise, the IC_{50} of 5-FU-Bi-QCS-AuNPs@collagen against A549 cells was 76.73 ± 3.8 µM compared to free 5-FU (478.64 ± 13.56 µM) as shown in Fig 29c. Therefore, it was concluded that the 5-FU loaded Bi-QCS-AuNPs@collagen significantly enhanced the anticancer activity of 5-FU toward HeLa and A549 cells up to 3.4-fold and 6.2-fold, respectively, compared to free 5-FU ($p < 0.05$). The enhancement of cancer inhibition results from the increase of intracellular uptake of 5-FU facilitated by the Bi-QCS-AuNPs@collagen. Positive charges (Quat188) in the modification of chitosan and the target molecule (biotin) play the critical role in delivering 5-FU into the cancer cells. Quat188 can enhance the electrostatic interactions with the negative charge of the cell membrane and the biotin can increase the cellular uptake by the biotin receptor-mediated endocytosis on the surface of cancer cells (Muddineti et al., 2015). After 5 - FU reaches the target cells, it exerts the anticancer effects through the inhibition of thymidylate synthase and the

incorporation of its active metabolites into RNA and DNA strands, which leads to apoptosis of the cancer cell [91].Consequently, Bi-QCS-AuNPs@collagen as nanocarriers is suitable for cancer treatments due to the increased efficacy and safety of anti-cancer drug delivery systems.

Figure 29 The cell viability of 5-FU and 5-FU-Bi-QCS-AuNPs@collagen in (a) HeLa and (b) A549 cell lines. (c) The IC$_{50}$ values of 5-FU and 5-FU-Bi-QCS-AuNPs@collagen in HeLa and A549 cell lines.

CHAPTER V

CONCLUSION

In this work, a novel modified chitosan/collagen biopolymer is used as a component for gold nanoparticle synthesis, stabilizer, and drug encapsulation enhancer. The collagen was used to synthesize gold nanoparticles through a reduction reaction, and the gold nanoparticle outer lay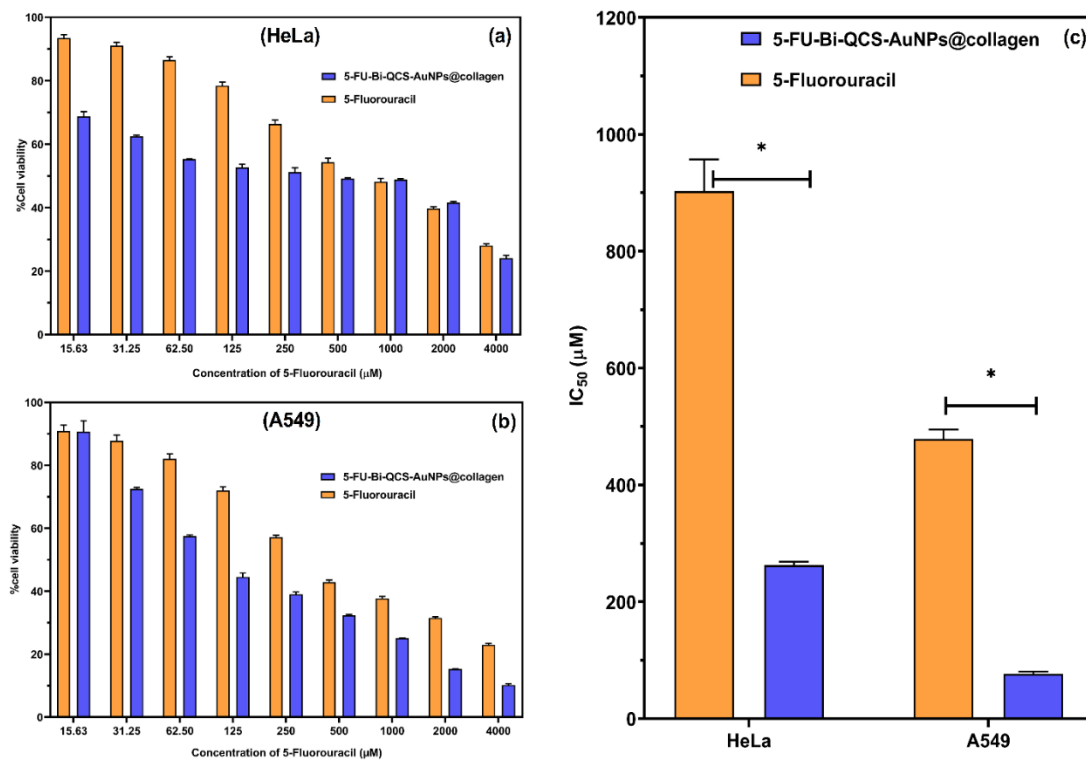er was coated with modified chitosan containing biotin molecules. Biotin as a target ligand exhibits targeting ability in cancer cells with overexpressed biotin receptors on the surface of cancer cells, especially lung cancer, and cervical cancer. The biocompatible chitosan/collagen gold nanoparticles clearly promoted tumor cell-targeting, prolong drug release, and have low cytotoxicity to normal cells in vitro. The physicochemical characters of the Biotin-Quat188-chitosan-AuNPs@collagen (Bi-QCS-AuNPs@collagen) were analyzed by ultraviolet–visible spectrophotometry (UV-vis), fourier-transform infrared spectroscopy (FTIR), transmission electron microscopy (TEM), dynamic light scattering (DLS), and zeta potential techniques. The average size of AuNPs@collagen particle was increased from 30 nm to 50 nm after coating with Bi-QCS. Moreover, the zeta potential of the nanoparticles was oppositely changed from -32.1 mV (uncoated) to 38.6 mV (coated with Bi-QCS), which confirmed the successful Bi-QCS coating of the nanoparticles. The encapsulation efficiency of 5-FU, determined by UV-vis spectrophotometry, was dramatically increased from 64.67% to 87.46% after the AuNPs@collagen were coated by the Bi-QCS due to strong electrostatic interactions and hydrogen bonding. It was also that Bi-QCS-AuNPS@collagen was a pH-sensitive nanoparticle, which could prevent premature release in a normal physiological pH but rapidly release the drug in an acidic condition in the tumor microenvironment.

Furthermore, the biological activities of Bi-QCS-AuNPs@collagen were studies. The Bi-QCS-AuNPs@collagen presented a significantly higher anti-inflammatory activity in RAW 264.7 macrophage cell line. The IC_{50} of the 5-FU-Bi-QCS-AuNPs@collagen was also evaluated in cervical (HeLa) and lung (A549) cancer cell lines. The Bi-QCS-AuNPs@collagen enhanced the activity of 5-FU approximately 3.3-fold and 6.2-fold in Hela and A549 cells respectively, compared with the free 5-Fluorouracil. According to these results, it was very promising that Bi-QCS-AuNPs@collagen could be translated to clinical applications for cancer treatments.

REFERENCES

1.   Patra, J.K., et al., *Nano based drug delivery systems: recent developments and future prospects.* Journal of Nanobiotechnology, 2018. **16**(1): p. 71.

2.   Tığlı Aydın, R.S. and M. Pulat, *5-Fluorouracil Encapsulated Chitosan Nanoparticles for pH-Stimulated Drug Delivery: Evaluation of Controlled Release Kinetics.* Journal of Nanomaterials, 2012. **2012**: p. 313961.

3.   Connor, E.E., et al., *Gold Nanoparticles Are Taken Up by Human Cells but Do Not Cause Acute Cytotoxicity.* Small, 2005. **1**(3): p. 325-327.

4.   Gao, X., et al., *In vivo cancer targeting and imaging with semiconductor quantum dots.* Nature Biotechnology, 2004. **22**(8): p. 969-976.

5.   Turkevich, J., P.C. Stevenson, and J. Hillier, *A study of the nucleation and growth processes in the synthesis of colloidal gold.* Discussions of the Faraday Society, 1951. **11**(0): p. 55-75.

6.   Frens, G., *Controlled Nucleation for the Regulation of the Particle Size in Monodisperse Gold Suspensions.* Nature Physical Science, 1973. **241**(105): p. 20-22.

7.   Anderson, M.J., et al., *One step alkaline synthesis of biocompatible gold nanoparticles using dextrin as capping agent.* Journal of Nanoparticle Research, 2011. **13**(7): p. 2843-2851.

8.   Tódor, I.S., et al., *Gold nanoparticle assemblies of controllable size obtained by hydroxylamine reduction at room temperature.* Journal of Nanoparticle Research, 2014. **16**(12): p. 2740.

9.   Marişca, O.T. and N. Leopold, *Anisotropic Gold Nanoparticle-Cell Interactions Mediated by Collagen.* Materials, 2019. **12**(7): p. 1131.

10.   Rana, S., et al., *Monolayer coated gold nanoparticles for delivery applications.* Advanced drug delivery reviews, 2012. **64**(2): p. 200-216.

11.   Zhang, L., et al., *Local anesthetic lidocaine delivery system: chitosan and hyaluronic acid-modified layer-by-layer lipid nanoparticles.* Drug Delivery, 2016. **23**(9): p. 3529-3537.

12. Jeon, S., C.Y. Yoo, and S.N. Park, *Improved stability and skin permeability of sodium hyaluronate-chitosan multilayered liposomes by Layer-by-Layer electrostatic deposition for quercetin delivery.* Colloids and Surfaces B: Biointerfaces, 2015. **129**: p. 7-14.

13. Mandapalli, P.K., et al., *Influence of charge on encapsulation and release behavior of small molecules in self-assembled layer-by-layer microcapsules.* Drug Delivery, 2014. **21**(8): p. 605-614.

14. Ariga, K., et al., *Layer-by-layer assembly for drug delivery and related applications.* Expert Opinion on Drug Delivery, 2011. **8**(5): p. 633-644.

15. Fuller, M. and I. KÖper, *Polyelectrolyte-Coated Gold Nanoparticles: The Effect of Salt and Polyelectrolyte Concentration on Colloidal Stability.* Polymers, 2018. **10**(12): p. 1336.

16. Hierrezuelo, J., et al., *Electrostatic stabilization of charged colloidal particles with adsorbed polyelectrolytes of opposite charge.* Langmuir, 2010. **26**(19): p. 15109-11.

17. Pino, P.d., et al., *Protein corona formation around nanoparticles – from the past to the future.* Materials Horizons, 2014. **1**(3): p. 301-313.

18. Slocik, J.M. and R.R. Naik, *Sequenced defined biomolecules for nanomaterial synthesis, functionalization, and assembly.* Current Opinion in Biotechnology, 2017. **46**: p. 7-13.

19. Vuola, J., et al., *Bone marrow induced osteogenesis in hydroxyapatite and calcium carbonate implants.* Biomaterials, 1996. **17**(18): p. 1761-1766.

20. Marisca, O.T., et al., *Comparison of the in Vitro Uptake and Toxicity of Collagen-and Synthetic Polymer-Coated Gold Nanoparticles.* Nanomaterials, 2015. **5**(3): p. 1418-1430.

21. Frank, L.A., et al., *Chitosan as a coating material for nanoparticles intended for biomedical applications.* Reactive and Functional Polymers, 2020. **147**: p. 104459.

22. Cha, J., et al., *Preparation and characterization of cisplatin-incorporated chitosan hydrogels, microparticles, and nanoparticles.* Macromolecular research, 2006. **14**(5): p. 573-578.

23. López-León, T., et al., *Physicochemical characterization of chitosan nanoparticles: electrokinetic and stability behavior.* Journal of Colloid and Interface Science, 2005. **283**(2): p. 344-351.

24. Darvishi, M.H., et al., *Novel biotinylated chitosan-graft-polyethyleneimine copolymer as a targeted non-viral vector for anti-EGF receptor siRNA delivery in cancer cells.* International Journal of Pharmaceutics, 2013. **456**(2): p. 408-416.

25. Hu, W., et al., *Biotin-Pt (IV)-indomethacin hybrid: A targeting anticancer prodrug providing enhanced cancer cellular uptake and reversing cisplatin resistance.* Journal of Inorganic Biochemistry, 2017. **175**: p. 47-57.

26. Liszbinski, R.B., et al., *Anti-EGFR-Coated Gold Nanoparticles In Vitro Carry 5-Fluorouracil to Colorectal Cancer Cells.* Materials, 2020. **13**(2): p. 375.

27. Shah, A., et al., *5-FU infusion in advanced colorectal cancer: a comparison of three dose schedules.* Cancer treatment reports, 1985. **69**(7-8): p. 739-742.

28. Caballero, G.A., R.K. Ausman, and J. Quebbeman, *Long-term, ambulatory, continuous IV infusion of 5-FU for the treatment of advanced adenocarcinomas.* Cancer Treat. Rep., 1985. **69**(1): p. 13-15.

29. Deng, Y., et al., *Application of the Nano-Drug Delivery System in Treatment of Cardiovascular Diseases.* Frontiers in Bioengineering and Biotechnology, 2020. **7**(489).

30. Wilczewska, A.Z., et al., *Nanoparticles as drug delivery systems.* Pharmacological Reports, 2012. **64**(5): p. 1020-1037.

31. Kateb, B., et al., *Nanoplatforms for constructing new approaches to cancer treatment, imaging, and drug delivery: what should be the policy?* Neuroimage, 2011. **54**: p. S106-S124.

32. Di Paolo, D., et al., *Drug delivery systems: application of liposomal anti-tumor agents to neuroectodermal cancer treatment.* Tumori Journal, 2008. **94**(2): p. 246-253.

33. Huynh, N.T., et al., *Lipid nanocapsules: a new platform for nanomedicine.* International journal of pharmaceutics, 2009. **379**(2): p. 201-209.

34. Yang, F., et al., *Liposome based delivery systems in pancreatic cancer treatment: from bench to bedside.* Cancer treatment reviews, 2011. **37**(8): p. 633-642.

35. Cho, K., et al., *Therapeutic nanoparticles for drug delivery in cancer.* Clinical cancer research, 2008. **14**(5): p. 1310-1316.

36. Peer, D., et al., *Nanocarriers as an emerging platform for cancer therapy.* Nature nanotechnology, 2007. **2**(12): p. 751-760.

37. Kamaly, N., et al., *Targeted polymeric therapeutic nanoparticles: design, development and clinical translation.* Chemical Society Reviews, 2012. **41**(7): p. 2971-3010.

38. Rawat, M., et al., *Nanocarriers: promising vehicle for bioactive drugs.* Biological and Pharmaceutical Bulletin, 2006. **29**(9): p. 1790-1798.

39. Madani, S.Y., et al., *A new era of cancer treatment: carbon nanotubes as drug delivery tools.* International journal of nanomedicine, 2011. **6**: p. 2963.

40. Medeiros, S., et al., *Stimuli-responsive magnetic particles for biomedical applications.* International journal of pharmaceutics, 2011. **403**(1-2): p. 139-161.

41. Fadeel, B. and A.E. Garcia-Bennett, *Better safe than sorry: understanding the toxicological properties of inorganic nanoparticles manufactured for biomedical applications.* Advanced drug delivery reviews, 2010. **62**(3): p. 362-374.

42. Vähä-Koskela, M.J., J.E. Heikkilä, and A.E. Hinkkanen, *Oncolytic viruses in cancer therapy.* Cancer letters, 2007. **254**(2): p. 178-216.

43. Hossen, S., et al., *Smart nanocarrier-based drug delivery systems for cancer therapy and toxicity studies: A review.* Journal of Advanced Research, 2019. **15**: p. 1-18.

44. Dykman, L. and N. Khlebtsov, *Gold nanoparticles in biology and medicine: recent advances and prospects.* Acta Naturae (англоязычная версия), 2011. **3**(2 (9)).

45. Chen, Y.-H., et al., *Methotrexate conjugated to gold nanoparticles inhibits tumor growth in a syngeneic lung tumor model.* Molecular pharmaceutics, 2007. **4**(5): p. 713-722.

46. Yaqoob, S.B., et al., *Gold, Silver, and Palladium Nanoparticles: A Chemical Tool for Biomedical Applications.* Frontiers in Chemistry, 2020. **8**(376).

47. Amina, S.J. and B. Guo, *A Review on the Synthesis and Functionalization of Gold Nanoparticles as a Drug Delivery Vehicle.* International Journal of Nanomedicine, 2020. **15**: p. 9823.

48. Wangoo, N., et al., *Synthesis and capping of water-dispersed gold nanoparticles by an amino acid: bioconjugation and binding studies.* Journal of colloid and interface science, 2008. **323**(2): p. 247-254.

49. Dong, J., et al., *Synthesis of precision gold nanoparticles using Turkevich method.* KONA Powder and Particle Journal, 2020. **37**: p. 224-232.

50. Brust, M., et al., *Synthesis of thiol-derivatised gold nanoparticles in a two-phase liquid–liquid system.* Journal of the Chemical Society, Chemical Communications, 1994(7): p. 801-802.

51. Du, Y. and B. Chen, *Combination of drugs and carriers in drug delivery technology and its development.* Drug design, development and therapy, 2019. **13**: p. 1401.

52. Zong, J., S.L. Cobb, and N.R. Cameron, *Peptide-functionalized gold nanoparticles: versatile biomaterials for diagnostic and therapeutic applications.* Biomaterials Science, 2017. **5**(5): p. 872-886.

53. Ramezani, F., et al., *Effect of peptide length on the conjugation to the gold nanoparticle surface: a molecular dynamic study.* DARU Journal of Pharmaceutical Sciences, 2015. **23**(1): p. 1-5.

54. Courrol, L.C. and R.A. de Matos, *Synthesis of gold nanoparticles using amino acids by light irradiation.* Catalytic Application of Nano-Gold Catalysts; Mishra, NK, Ed.; IntechOpen: London, UK, 2016: p. 83-99.

55. PreparingToBecome.LLC. *The amino acid, Peptide, and Protein.* 2021 [cited 2021 May 08]; Available from: https://preparingtobecome.com/amino-acids-peptides-and-proteins/.

56. Liu, B. and J. Liu, *Interface-Driven Hybrid Materials Based on DNA-Functionalized Gold Nanoparticles.* Matter, 2019. **1**(4): p. 825-847.

57. Fuller, M.A. and I. Köper, *Biomedical applications of polyelectrolyte coated spherical gold nanoparticles.* Nano Convergence, 2019. **6**(1): p. 11.

58. Hierrezuelo, J., et al., *Electrostatic stabilization of charged colloidal particles with adsorbed polyelectrolytes of opposite charge.* Langmuir, 2010. **26**(19): p. 15109-15111.

59. Moore, T.L., et al., *Nanoparticle colloidal stability in cell culture media and impact on cellular interactions.* Chem Soc Rev, 2015. **44**(17): p. 6287-305.

60. Fuller, M.A. and I. Köper, *Biomedical applications of polyelectrolyte coated spherical gold nanoparticles.* Nano convergence, 2019. **6**(1): p. 1-10.

61. Pham, S., Y.H. Choi, and J. Choi, *Stimuli-Responsive Nanomaterials for Application in Antitumor Therapy and Drug Delivery.* Pharmaceutics, 2020. **12**: p. 630.

62. Pham, S.H., Y. Choi, and J. Choi, *Stimuli-Responsive Nanomaterials for Application in Antitumor Therapy and Drug Delivery.* Pharmaceutics, 2020. **12**(7): p. 630.

63. Sun, T., et al., *Engineered nanoparticles for drug delivery in cancer therapy.* Angewandte Chemie International Edition, 2014. **53**(46): p. 12320-12364.

64. Conner, S.D. and S.L. Schmid, *Regulated portals of entry into the cell.* Nature, 2003. **422**(6927): p. 37-44.

65. Cartiera, M.S., et al., *The uptake and intracellular fate of PLGA nanoparticles in epithelial cells.* Biomaterials, 2009. **30**(14): p. 2790-2798.

66. Decuzzi, P. and M. Ferrari, *The role of specific and non-specific interactions in receptor-mediated endocytosis of nanoparticles.* Biomaterials, 2007. **28**(18): p. 2915-2922.

67. Koli, U., et al., *Lung Cancer Receptors and Targeting Strategies*, in *Targeted Intracellular Drug Delivery by Receptor Mediated Endocytosis*, P.V. Devarajan, P. Dandekar, and A.A. D'Souza, Editors. 2019, Springer International Publishing: Cham. p. 229-268.

68.   Shevtsov, M., H. Gao, and G. Multhoff, *Membrane heat shock protein 70: A theranostic target for cancer therapy.* Philosophical Transactions of the Royal Society B: Biological Sciences, 2018. **373**: p. 20160526.

69.   Mao, Z., X. Zhou, and C. Gao, *Influence of structure and properties of colloidal biomaterials on cellular uptake and cell functions.* Biomaterials Science, 2013. **1**(9): p. 896-911.

70.   Luesakul, U., et al., *Quaternized chitosan-coated nanoemulsions: A novel platform for improving the stability, anti-inflammatory, anti-cancer and transdermal properties of Plai extract.* Carbohydrate Polymers, 2020. **230**: p. 115625.

71.   Yao, Q., et al., *Preparation and characterization of biotinylated chitosan nanoparticles.* Yao xue xue bao= Acta pharmaceutica Sinica, 2007. **42**(5): p. 557-561.

72.   Singh, P., et al., *Pharmacological importance, characterization and applications of gold and silver nanoparticles synthesized by Panax ginseng fresh leaves.* Artificial cells, nanomedicine, and biotechnology, 2016. **45**: p. 1-10.

73.   Medhe, S., P. Bansal, and M.M. Srivastava, *Enhanced antioxidant activity of gold nanoparticle embedded 3,6-dihydroxyflavone: a combinational study.* Applied Nanoscience, 2014. **4**(2): p. 153-161.

74.   Lee, R.J. and P.S. Low, *Folate-mediated tumor cell targeting of liposome-entrapped doxorubicin in vitro.* Biochimica et Biophysica Acta (BBA)-Biomembranes, 1995. **1233**(2): p. 134-144.

75.   Sangthong, S., et al., *Anthracene-9, 10-dione derivatives induced apoptosis in human cervical cancer cell line (CaSki) by interfering with HPV E6 expression.* European Journal of Medicinal Chemistry, 2014. **77**: p. 334-342.

76.   Sajomsang, W., et al., *Quaternization of N-aryl chitosan derivatives: synthesis, characterization, and antibacterial activity.* Carbohydrate Research, 2009. **344**(18): p. 2502-2511.

77.   Balan, V., et al., *Biotinylated N-palmitoyl chitosan for design of drug loaded self-assembled nanocarriers.* European Polymer Journal, 2016. **81**: p. 284-294.

78. Noruzi, M., et al., *Rapid green synthesis of gold nanoparticles using Rosa hybrida petal extract at room temperature.* Spectrochimica Acta Part A: Molecular and Biomolecular Spectroscopy, 2011. **79**(5): p. 1461-1465.

79. Laksee, S., et al., *Facile and green synthesis of pullulan derivative-stabilized Au nanoparticles as drug carriers for enhancing anticancer activity.* Carbohydrate Polymers, 2018. **198**: p. 495-508.

80. Maruyama, T., Y. Fujimoto, and T. Maekawa, *Synthesis of gold nanoparticles using various amino acids.* J Colloid Interface Sci, 2015. **447**: p. 254-7.

81. Maeda, H., et al., *Tumor vascular permeability and the EPR effect in macromolecular therapeutics: a review.* J Control Release, 2000. **65**(1-2): p. 271-84.

82. Song, K., et al., *Smart gold nanoparticles enhance killing effect on cancer cells.* International journal of oncology, 2013. **42**(2): p. 597-608.

83. Dhinasekaran, D., et al., *Chitosan mediated 5-Fluorouracil functionalized silica nanoparticle from rice husk for anticancer activity.* International Journal of Biological Macromolecules, 2020. **156**: p. 969-980.

84. Unsoy, G., et al., *Synthesis of Doxorubicin loaded magnetic chitosan nanoparticles for pH responsive targeted drug delivery.* Eur J Pharm Sci, 2014. **62**: p. 243-50.

85. Guzik, T., R. Korbut, and T. Adamek-Guzik, *Nitric oxide and superoxide in inflammation.* J physiol pharmacol, 2003. **54**(4): p. 469-487.

86. Guha, M. and N. Mackman, *LPS induction of gene expression in human monocytes.* Cell Signal, 2001. **13**(2): p. 85-94.

87. Chen, Y.-P., et al., *Antioxidant and anti-inflammatory capacities of collagen peptides from milkfish (Chanos chanos) scales.* Journal of Food Science and Technology, 2018. **55**(6): p. 2310-2317.

88. Gu, X., et al., *Pinocembrin attenuates allergic airway inflammation via inhibition of NF-κB pathway in mice.* International Immunopharmacology, 2017. **53**: p. 90-95.

89. Kim, M.S., et al., *Inhibitory effect of water-soluble chitosan on TNF-alpha and IL-8 secretion from HMC-1 cells.* Immunopharmacol Immunotoxicol, 2004. **26**(3): p. 401-9.

90. Júnior, R., et al., *Anti-inflammatory, analgesic and anti-tumor properties of gold nanoparticles.* Pharmacological reports: PR, 2016. **69**.

91. Pan, X., et al., *Autophagy Inhibition Promotes 5-Fluorouraci-Induced Apoptosis by Stimulating ROS Formation in Human Non-Small Cell Lung Cancer A549 Cells.* PloS one, 2013. **8**: p. e56679.

VITA

NAME	Miss Naruthai Hongsa
DATE OF BIRTH	27 September 1995
PLACE OF BIRTH	Ranong
INSTITUTIONS ATTENDED	Bachelor Degree in Chemistry from Thaksin University, 2015-2018
	Master Degree of Chemistry, Faculty of Science, Chulalongkorn University, 2019-2021
HOME ADDRESS	153/37 Bangnaisee ,Takuapa, Phang-nga, 82110